remote sensing

MDPI

Review

A Review of Crop Water Stress Assessment Using Remote Sensing

Uzair Ahmad *, Arturo Alvino and Stefano Marino

Department of Agricultural, Environmental and Food Sciences (DAEFS), University of Molise, 86100 Campobasso, Italy; alvino@unimol.it (A.A.); stefanomarino@unimol.it (S.M.)
* Correspondence: u.ahmad@studenti.unimol.it or druzair94@gmail.com; Tel.: +39-380-490-6654

Abstract: Currently, the world is facing high competition and market risks in improving yield, crop illness, and crop water stress. This could potentially be addressed by technological advancements in the form of precision systems, improvements in production, and through ensuring the sustainability of development. In this context, remote-sensing systems are fully equipped to address the complex and technical assessment of crop production, security, and crop water stress in an easy and efficient way. They provide simple and timely solutions for a diverse set of ecological zones. This critical review highlights novel methods for evaluating crop water stress and its correlation with certain measurable parameters, investigated using remote-sensing systems. Through an examination of previous literature, technologies, and data, we review the application of remote-sensing systems in the analysis of crop water stress. Initially, the study presents the relationship of relative water content (RWC) with equivalent water thickness (EWT) and soil moisture crop water stress. Evapotranspiration and sun-induced chlorophyll fluorescence are then analyzed in relation to crop water stress using remote sensing. Finally, the study presents various remote-sensing technologies used to detect crop water stress, including optical sensing systems, thermometric sensing systems, land-surface temperature-sensing systems, multispectral (spaceborne and airborne) sensing systems, hyperspectral sensing systems, and the LiDAR sensing system. The study also presents the future prospects of remote-sensing systems in analyzing crop water stress and how they could be further improved.

Keywords: crop water stress; hyperspectral; LiDAR; multispectral; optical sensing; remote sensing; sentinel-1; soil moisture; thermometric sensing

Citation: Ahmad, U.; Alvino, A.; Marino, S. A Review of Crop Water Stress Assessment Using Remote Sensing. *Remote Sens.* **2021**, *13*, 4155. https://doi.org/10.3390/rs13204155

Academic Editors: Abdelghani Chehbouni, Salah Er-Raki and Wenquan Zhu

Received: 9 September 2021
Accepted: 14 October 2021
Published: 17 October 2021

1. Introduction

Irrigation water is considered a fundamental and vital resource for agricultural production [1]. A lack of irrigation water will result in crop water stress occurring at different crop stages and under different environmental conditions, whereby the effects on crop and soil characteristics manifest in a diverse manner. The primary effect is experienced in the photosynthesis rate, which further leads to disruption of the transpiration rate. Arid regions have determined innovative ways to fulfill their crop needs according to their growth stages, type, and environmental conditions, which results in significant improvements in yield [2,3]. Providing more or less irrigation than required ultimately damages crop growing length and yield production in addition to causing other problems.

Remote-sensing technology, since its initiation, has come to benefit agriculture in many ways [4]. It has simplified and optimized agricultural farming [5] through the rapid detection of crop biomass changes that are often overlooked by traditional methods [6]. Remote sensing utilizes different technologies that are based on computer applications to gather data from crop, soil, and environmental factors and without physical contact (Figure 1) [7]. The remote-sensing system provides specific information useful in the analysis of irrigation scheduling, amount, and time, and determines crop temperature with high precision [8].

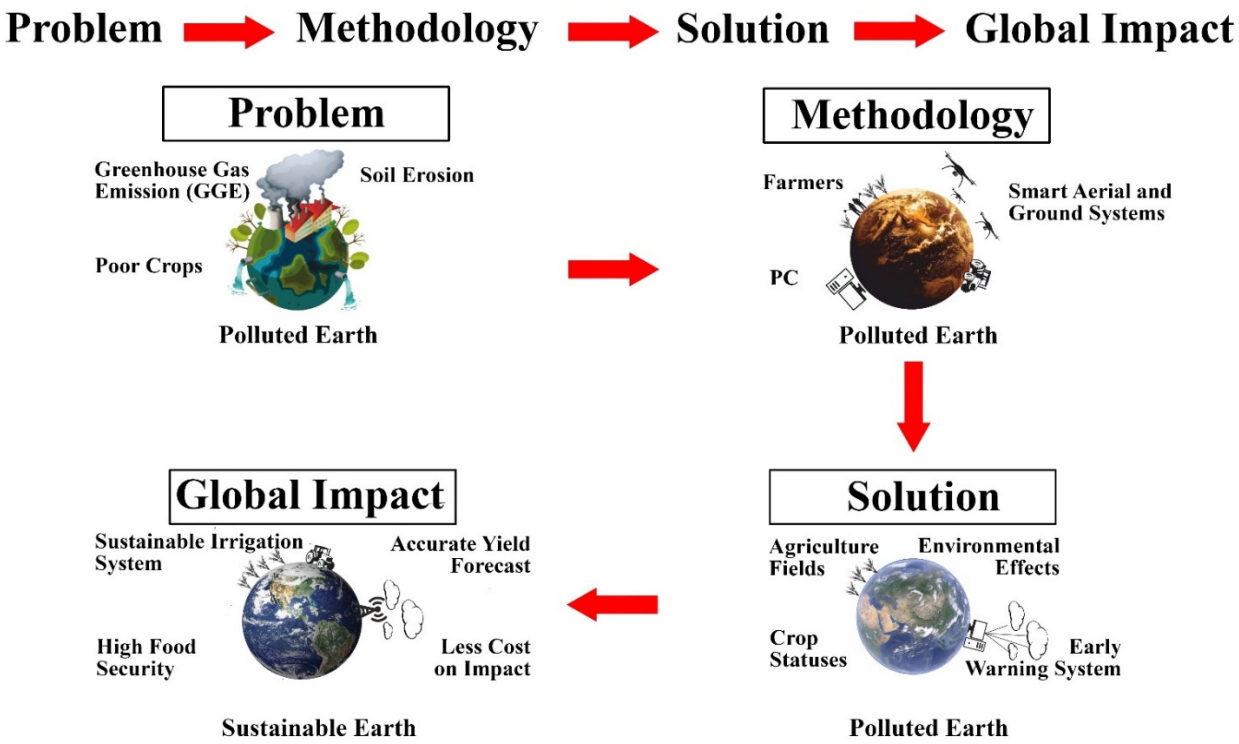

Figure 1. The graphical abstract visualizes the remote-sensing technology that perfectly addresses crop water stress using crop statistics and computer software by (1) identifying the problem, (2) implementing the methodology, (3) delivering the solution, and (4) addressing global crop water stress.

Crop water stress (CWS) assessment is one of the factors that define the environmental interaction of a crop and is a prerequisite for performing precision irrigation scheduling [9]. CWS is defined as "an indicator that determines water deficit condition based on the scale of the leaf and the crop temperature analysis method". The CWS, which was developed by Idso et al. [10], was later considered a standard indicator to assess the stress at the leaf and canopy scales. This was an improvement of the standardized procedure for assessing plot and regional scale water stress, including evapotranspiration, at a larger scale. The standardized method potentially addressed the stress effects by analyzing the relationship between TIR and NIR-SWIR as an indicator of vegetation water availability [11,12]. Based on the standardized method, Khorsand et al. [13] reported critical limitations of leaf and canopy scales and of their relationship within diverse environmental conditions. The study utilized the regression baseline model and found CWS values of 0.37 and 0.15 for different leaf- and canopy-level scales. The study further showed that the regression baseline method for leaf and canopy scales can provide significant results for application in long-term forecasting (Figure 2). The regression baseline model can be readily used to provide CWS status and simplifies the analysis of crop variety, soil type, and environmental factors.

This critical review examined the analysis of crop water stress using remote-sensing systems. Initially, the relationship of relative water content (RWC) with equivalent water thickness (EWT) and soil moisture crop water stress is determined. Evapotranspiration and sun-induced chlorophyll fluorescence are then analyzed in relation to crop water stress using remote-sensing systems. Finally, the study presents an overview of remote-sensing technologies used to detect crop water stress, including optical sensing systems, thermometric sensing systems, land-surface temperature-sensing systems, multispectral (spaceborne and airborne) sensing systems, hyperspectral sensing systems, and the LiDAR sensing system.

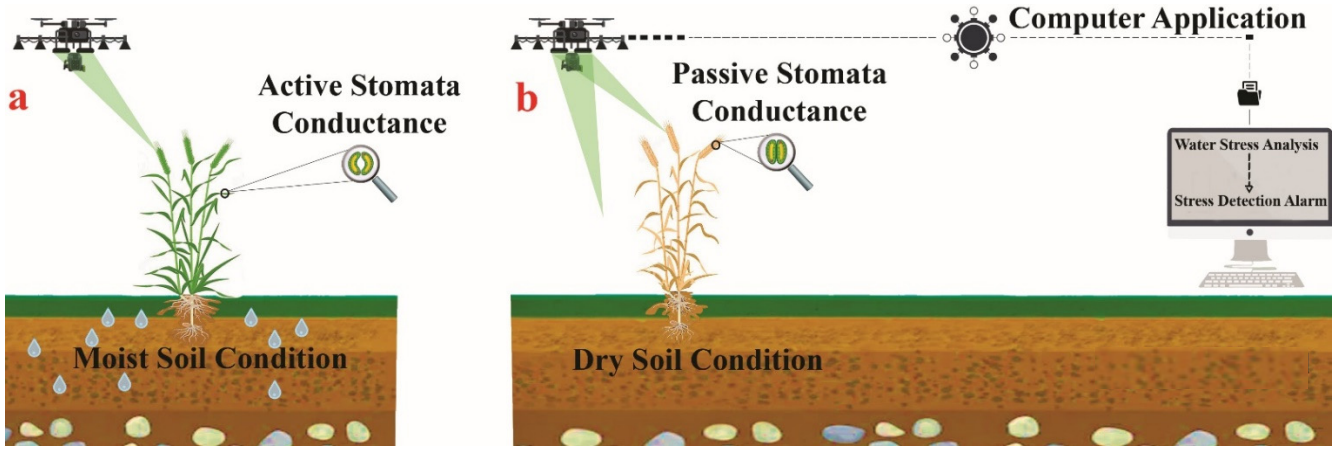

Figure 2. Crop water stress assessment: (**a**) Normal stomatal conductance with no stress retrieved, (**b**) comparison of irrigation water resources and micro-environmental conditions near the plant source to evaluate the intensity of the crop water stress content in real-time field conditions.

The aims of our study are to:

(i) Summarize the current scope of crop water stress detection using remote-sensing technology.
(ii) Present real-world examples and relevant methods.
(iii) Classify common features of crop water stress used in detection to benefit the literature on this topic.

2. Relative Water Content and Crop Water Stress

Inoue et al. [14] defined the relative water content (RWC) as the ratio of the available quantity of soil moisture and crop water. The study further specified the RWC as

$$\text{RWC} = (\text{fresh weight} - \text{dry weight})/(\text{turgid weight} - \text{dry weight})$$

where:

FW = fresh weight (%);
DW = dry weight (%);
TW = turgid weight (%).

Crop RWC is an important parameter in acquiring a crop's physiological status [15,16], biochemical status [17–20], and irrigation use efficiency [21–24]. Thanks to remote-sensing systems, these conditions can be effectively tracked for leaf water potential and moisture availability for effective and timely measures [25].

RWC can be determined with high accuracy using spectral remote-sensing systems, whereby spectral data are analyzed to provide simple readable information. Qi et al. [26], for example, successfully used remote-sensing spectral systems to acquire accurate RWC data in a timely manner. The equivalent water thickness (EWT) of a leaf is used to assess RWC, which provides the available water quantity per unit leaf area [27], with which researchers can then determine the level of stress that the leaf experiences or will experience in the future. This remote-sensing technique can precisely quantify crop water stress based on leaf measurements, which is vital in making certain decisions.

The quantity of solar radiation received also affects crop EWT. EWT is related to crop leaf moisture. Under high solar radiation, the water requirement is high, so a high amount of water is absorbed and transpired [28]. EWT, as determined with remote sensors, can be used to analyze crop water demand and moisture availability. The remote-sensing sensors continuously monitor EWT assessment values (low and high), which, in extreme cases, lead to crop death, whereas a rapid increase and positive values reveal minor crop water stress. De Jong et al. [29] presented EWT values determined using a spectral remote-sensing

system at three locations, where a good correlation of 0.70 was found between leaf water content and spectral indices at the 970 nm wavelength band.

The EWT approach [29] for determining water weight (FW − DW) per the leaf area index (LAI) is expressed as

$$EWT = (FW - DW)/LAI$$

For determining crop water stress at the RWC level, understanding the leaf water content is important. The correlation with leaf water content is determined using a remote-sensing system [30]. Ceccato et al. [31], Wang et al. [32], and Zhang et al. [33] stated that leaf water content stress and low water potential are created through an imbalance. The imbalance appears when the evaporated leaf water content and absorbed water level (by the root system) are not equal. Leaf water stress depends on the plant condition. Its transpiration rate and temperatures are indirectly related to each other. In conditions of higher transpiration, low crop water stress is due to the water availability of the leaves, while low transpiration leads to high crop water stress (Figure 3) [34]. The transpiration rate, temperature, cooling, and heating effects are detected by remote-sensing systems and further processed for crop water stress assessment [35]. However, the methods for leaf water content estimation are overly time-consuming and are not considered efficient for large-scale spatial analysis. For limited spatial analysis, modern remote-sensing methods provide useful results [36]. Among them is a canopy temperature remote-sensing method that has attracted considerable attention for characterizing crop water stress [37].

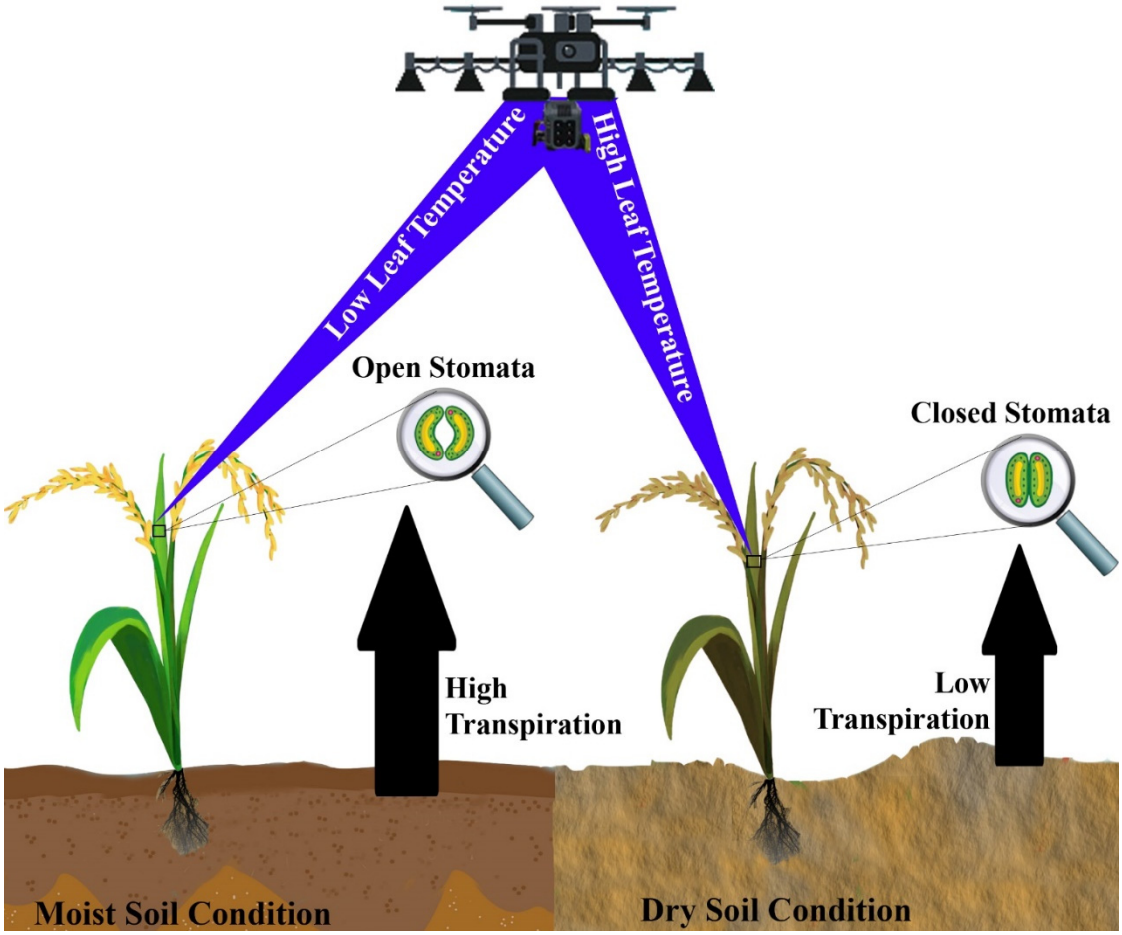

Figure 3. Remote-sensing estimation of the crop water stress using leaf transpiration, temperature, cooling, and heating effects, and comparing it with the air and soil moisture levels.

Leaves are not considered a real representative of the complete canopy but are the top portion of the plant that receives direct solar radiation. This quantity of absorbed solar radiation influences crop parameters, such as leaf area index (LAI) and upper and lower leaf features, which are significant characteristics in the remote determination of RWC. Tanner [38] developed a system for studying canopy temperature in order to continuously monitor RWC. His study provided an overview of leaf temperature and explains how a single leaf is not capable of representing the entire canopy. This minimizes the need for a specialized system and high-cost maintenance, and less time is needed for analysis [39]. This opened up new ways to automatically monitor RWC stress. However, the lack of availability of a diverse set of factors [40], decreased sensor image quality [41], and high costs [42] are issues of the system that still need to be addressed. As crop RWC is affected by soil moisture, the RWC is overestimated under conditions of high soil moisture, while at low soil moisture, the RWC is underestimated. Both RWC and soil moisture are interdependent variables, and little research has been conducted on their effects on crop water stress [43,44]. A study conducted a model based on a linear relationship between NDVI reflectance and soil moisture. It estimated a linear relationship between root zone soil moisture and leaf water potential, but the test was conducted at a depth of 0–5 cm [25]. In this context, the following section examines the relationship of soil moisture with its interdependent variables.

Satellite systems such as soil moisture active passive (SMAP) and soil moisture and ocean salinity (SMOS) use passive signals to assess soil moisture. The L-band frequency measured by these systems can be used to map the global near-surface (0–5 cm) soil moisture with optimum spatial (25–40 km) and temporal resolution (2–3 d). They are further able to analyze the near-surface soil moisture content up to the crop root zone (top 1 m) by using data assimilation methods and processing models [45]. The function of these systems is to monitor the soil moisture at various locations and sparse monitoring chains and to perform analysis.

Initial research on SMAP and SMOS soil moisture analysis showed significant correlations between the equipment tested in previous years, but there were differences found in extreme temperatures such as hot and cold zones due to variations in equipment, structure, and algorithms [46]. The Sentinel-1 mission was tested using the SMAP system for their overlapping orbits, system functions, and temporal conductivity. This analysis provided advancement in the soil moisture data for global coverage. Various modern satellites (active and passive) and sensors have started acquiring data for soil moisture. Soil moisture data with advanced spatial resolution have been acquired by Sentinel-1 and the ALOS-2 PALSAR satellite mission with a 10 m resolution [47]. Previous satellite systems provided a revisit frequency of 14 days that is not efficient for soil moisture analysis [48–50].

Soil moisture spatiotemporal analysis is conducted by the Sentinel-1 system. The system further recommends potential processes for relative content analysis. Paloscia et al. [51] and Hornacek et al. [52] reported on Sentinel-1 as the first soil moisture data analyzer. Table 1 shows the latest L-band missions, including the National Aeronautics and Space Administration (NASA), USA, the Indian Space Research Organization (ISRO), the synthetic aperture radar (SAR—collectively referred to as NISAR), and the German-based Tandem-L missions [53], which provided valuable datasets of soil moisture determination at a high spatial resolution, giving rise to further novel satellite missions. The German-based Tandem-L mission was used on two sets of radar satellites that operate in the L-band module. The system is considered highly efficient for the global monitoring of dynamic developments on the soil surface, including the crop vegetation's vertical structure, soil surface temperature, and soil surface distortion. The NISAR mission is based on a dual frequency (S and L bands) with the synthetic space radar to understand natural developments of the soil, such as environmental progressions.

Bogena et al. [54] reported on non-invasive remote-sensing systems for the determination of soil moisture. Particularly, the cosmic ray soil moisture interaction code (COSMIC) and the cosmic ray neutron probe (CRNP) showed promising results in acquiring soil

moisture. The system analyzed the tested area from a few hundred to a thousand square meters at a single time. The soil moisture map was estimated by a study using the SAtélite de Observación COn Microondas (SAOCOM) mission. The soil moisture sampling work consists of 17–20 nodes with 44 total measurement sites in order to cover the spatial variability of the soil moisture of the large area. The objective of the studies was to analyze the number of surface soil moisture samples required to determine the areal mean, which showed 95% accuracy and 3% *v/v* error bounds in all nine fields. Results showed an acceptable level of accuracy between the tested parameters and satellite data, with no significant differences [55]. Additionally, various soil moisture test locations including sensors with diverse levels of precision and accuracy, such as the German-based terrestrial environmental observatories (TERENO), the US-based Marena Oklahoma in situ sensor testbed (MOISST), and the US-based Texas soil observation network (TxSON), were tested in the analysis of soil moisture content.

Table 1. Satellites that monitor global soil moisture content with major applications and their respective advantages and disadvantages.

Systems	Application	Advantages	Limitations	References
AMSR-2	Global observation of soil moisture (from the soil surface to a few cm depth), soil water-related parameter analysis	Acquires both day- and night-time data with more than 99% accuracy/Good acquisition of the resolution and accuracy of the data collection	Works only at specific frequency bands, such as 6.925, 7.3, 10.65, 18.7, 23.8, 36.5, and 89.0 GHz	[56]
AMSR-E	Passive microwave soil moisture analysis with high efficiency in relation to drought	Acquisition of daily determination of soil moisture data with precise resolution of 12.5 km	Only two files per day, one daytime and one nighttime	[57]
NISAR	Spatially based maps of global soil moisture in 6–12 days	Acquires day/night and all-weather for soil moisture data with precise resolution of 3–10 m	Product evaluation in 12–24 h	[58]
Tandem-L	Global soil moisture	Provides highly precise measured data ranging within a millimeter accuracy with precise resolution from 20 m to 4 km	Much more expensive than traditional satellite systems	[59]
Sentinel-1	Dynamics observation	Field determination is less accurate with precision resolution from 5 to 20 m	Easy to develop new systems, including application development models and sensor structures	[60]
SMAP	Analyze soil surface and vegetation status	High chance of mission failure with the precision resolution of 9 km	Passive sensors acquire SSM for about 36 km	[61]

3. Evapotranspiration and Crop Water Stress

Evapotranspiration (ET) is the water quantity lost to the atmosphere from the crop's stomatal aperture and transpiration. Irrigation water availability is a major determinant of ET, which can be used at different levels. A previous study examined these processes, and Allen et al. [62] determined various techniques and presented empirical approaches in analyzing the evapotranspiration with the help of different environmental parameters [63]. This study was tested by many researchers and agronomists under different climatological conditions and proved to be a good approach in analyzing crop water stress with energy exchanges. In some climatological conditions, the crop coefficient (Kc) shows a variable and distant approach for determining real-time crop growth. To avoid issues, techniques have been further updated by including the weather-dependent references ET and Kc, which further specifies the type and production stage of the crop.

López-López et al. [64] analyzed the crop evapotranspiration (ETc) for soil matrix potential and validated crop water stress with the help of an infrared ray gun as a remote-sensing tool. Researchers revealed that values ranging from 1.21 to 1.31 VPD could be recorded in crops with lower water stress, with an r^2 of 0.68. Marino et al. [65] investigated the effects of different irrigation levels on the physiological responses of crops and found that the seasonal reference evapotranspiration was 252.4 mm, while that of crop evapotranspiration was 194.3 mm using remote-sensing-based UAV systems.

In many cases, the crop growing stage cannot be observed by growers in field conditions. In these particular conditions, satellites provide spatially uniform data to diversify crop growth stages by analyzing evapotranspiration. This is performed by the METRIC modeling of imagery data acquired by the remote-sensing method. The METRIC model is based on the term SEBAL, which works via the energy balance method for crop water stress assessment using remote sensing.

Alghory et al. [66] determined crop water stress using an evapotranspiration analysis. Tests showed that an irrigation deficit could potentially benefit crop yield. Other studies defined empirical approaches to determine crop water stress [67–69], where the ET of crops was analyzed using remote-sensing systems. Sun et al. [70] and Shellie et al. [71] examined the auto-model system for crop water stress estimation. Studies revealed that, upon minimizing half of the irrigation quantity, the recorded ETc was 70–35% of the original values, whereas the studies recorded the particular crop water stress index at 0.4–0.6.

Romero-Trigueros et al. [72] and Akkuzu et al. [73] analyzed the crop water stress index using a thermal remote-sensing system and found values ranging from 0 to 0.68 and from 0.02 to 0.71 in different years. Dauphin [74] (Figure 4) validated NASA's Ecosystem Spaceborne Thermal Radiometer, called ECOSTRESS, to evaluate evapotranspiration and ultimately assess crop water stress for different crops in Peru. The study concluded that some regions recorded low evapotranspiration and high crop water stress.

Dauphin et al. [74] studied Moderate–Resolution Imaging Spectroradiometer (MODIS) imagery that provides maps of global agricultural production and conditions influencing global food security on a timely and regular basis. The Global Land Evaporation Amsterdam Model (GLEAM) is a collection of algorithms that separately estimate the evaporation, transpiration, bare–soil evaporation, interception loss, open–water evaporation, and sublimation. The system was developed to maximize the recovery of data on evaporation contained in the latest satellite observations of environmental and climatic variables. The system provides three salient features: (1) Consideration of the soil moisture parameter on evaporation, (2) a thorough analysis of forest interception, and (3) wide utilization of microwave recordings, which offer an advantage in cloudy conditions [75]. Remote–sensing systems have a unique capacity to analyze crop water stress. The systems that use spectral bands provide efficient, accurate, and optimum evapotranspiration for the estimation of crop water stress. Gerhards et al. [76] revealed that, upon providing complete irrigation to crops, crop water stress in crop production was guaranteed at the crop maturity stage. With the proper availability of soil moisture, crop water stress was 0.2. This showed the

benefits of crop water stress detection, whereby the greater the crop water stress, the lower the crop yield.

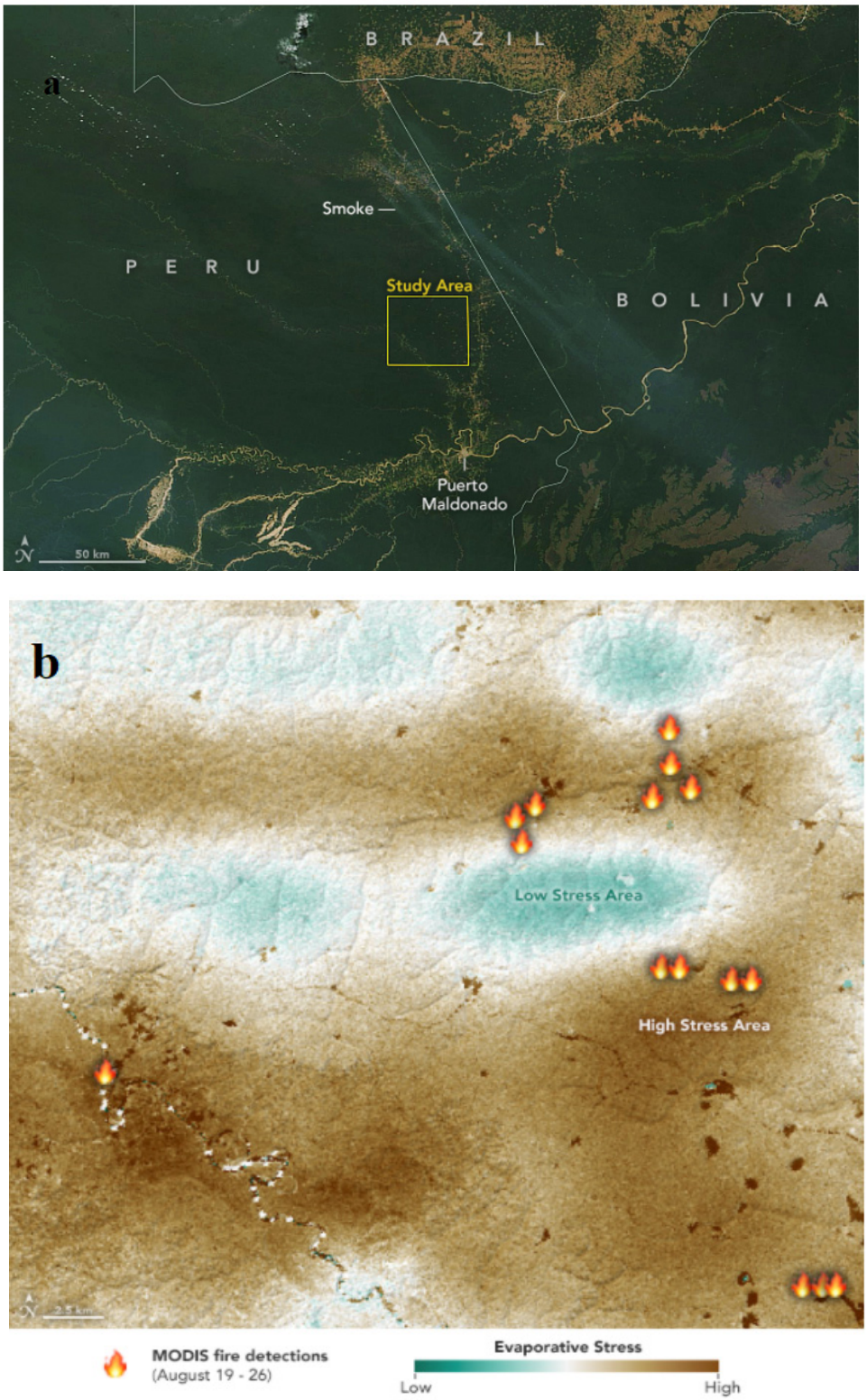

Figure 4. Evapotranspiration stress by Terra satellite of NASA's MODIS system and Ecostress system in east Peru. (**a**) Study area of the conducted tests, and (**b**) crop water stress from high to mid and low [74].

4. Sun–Induced Chlorophyll Fluorescence and Crop Water Stress

Studies show that remote–sensing systems provide a precise analysis of deep machine learning [2,77,78], which comes from the target object and evaluates photosynthetic, biotic, abiotic, and nutrient processes using both passive and active methods to monitor crop water stress [79]. The passive analysis is linked with chlorophyll fluorescence emissions and is considered a good indicator of the photosynthetic potential. Passive methods are used to measure the sun–induced chlorophyll fluorescence (SIF) that is produced from the vegetation source in the form of a photosynthetic light reaction after sunlight is absorbed by the leaf. This provides a direct assessment of the photosynthetic process [80] and spectral resolution data [81]. They are based on the total emitted fluorescence values, but the values acquired by SIF are lower in field conditions. SIF ranges from 1.0 to 3.5% of the shortwave energy gained from solar radiation and is determined in a specific spectral wavelength with a shorter amount of solar irradiation values [82].

Different methods have been used to determine SIF. One important method is the Fraunhofer line depth (FLD), which is based on specific bands of solar radiation absorbed by the source plant [83], based on the canopy and ecosystem level. Spaceborne systems perform global SIF procedures and store the acquired data in a safe database. These systems were initially developed to measure atmospheric procedures; however, researchers have since developed specific algorithms that now measure the SIF.

The sensor of the system ranges from a tropospheric monitoring instrument (TROPOMI), an orbiting carbon observatory (OCO), Global Ozone Monitoring Experiment 2 (GOME–2) instruments, and a scanning imaging absorption spectrometer for atmospheric cartography (SCIAMACHY) [84]. The TROPOMI/GOME–2 fluorescence retrievals illustrate a similar spatial structure as compared with those from a simpler method applied to the Greenhouse gases Observing Satellite (GOSAT). The system provides a global analysis of far–red fluorescence with a higher resolution at smaller spatial and temporal scales. Near–global coverage is delivered within a few days. Studies have shown the physically plausible variations in chlorophyll over the time period of a single month at a spatial resolution of $0.5^\circ \times 0.5^\circ$. Results provided significant differences between chlorophyll fluorescence and NDVI retrievals [85]. Further investigations about SIF are being carried out by the European Space Agency, which developed a mission known as the fluorescence explorer (FLEX) for 2023. The FLEX mission is expected to provide high–resolution spectrometric data for global SIF mapping and the rapid determination of visible, red, and near–infrared reflectance [86].

SIF is estimated by using slight absorption lines received from the solar irradiance range (Fraunhofer lines) between 650 and 800 nm, and Earth's atmosphere absorption lines are also utilized [83]. The classical method to retrieve SIF is the sub–nanometer spectral resolution between 760.5 and 687.5 nm [87].

Studies reported that SIF is an efficient optical indication of leaf and crop water stress [88] and have validated the use of SIF in evaluating leaf stress; however, the potential for utilizing this relationship is still not fully understood for the canopy level [89,90]. Because of this, studies related to SIF in red (FR) and far red (FFR) bands are potentially useful for tracking crop water stress [91]. A comprehensive analysis of the SIF temporal variable is required to understand stress levels. SIF and the photosynthetic relationship need to be further analyzed to assess their application in determining crop water stress [92–96].

5. Optical Sensing Systems and Crop Water Stress

Wheat yield is affected by the grain number per grain filling, which is considered a dominant factor compared to senescence [97]. However, research using optical sensing systems revealed a positive correlation between yield and delayed senescence under crop water stress [98]. An optical sensing system records green phenotypic status as a determinant of crop water stress and analyzes premature senescence [99]. Senescence is therefore a vital standard in observing crop vegetation using optical sensing systems when

considering regions with high weather variation, with more frequent and severe droughts and high temperatures.

Optical sensing systems provide optimized senescence dynamics that intensify field tests for various reasons: (i) Senescence in itself is identified and can be indicative of environmental variations as an underlying cause [100], which ultimately results in low to moderate heritability in stress conditions [101]; (ii) senescence impacts yield parameters and protein content and can be caused by crop water stress [102]. The sensitivity of an optical sensing system can determine stress conditions affecting yield parameters and green factors. Optical sensing systems can be used to determine the nature of crop water stress, which is a relevant problem; in fact, various stress factors impose similar effects on crops. Crop water stress alters the senescence effects on crops, which leads to the removal or reduction of specific senescence properties [103].

An analysis of efficient senescence provides precise crop water stress using the optical sensor system, which has positive effects on the harvest index [104], yield protein, and nitrogen use efficiency [105]. Yield protein is a standard factor in vegetation production, which is affected by the dilution quantity under the condition of increased C–compound synthesis [106]. Thus, for exploiting differences in senescence for the determination of crop water stress using optical sensor systems, concrete knowledge of the vegetation genetics, environments, and physiological factors of senescence and their correlations under crop water stress conditions need to be investigated.

An optical sensing system can be used for the detection of various crop stress–resistance mechanisms [97]. Vegetation crops have benefited from such mechanisms in avoiding crop water stress. One such mechanism is stomatal conductance (opening and closure), which can be monitored. This system shows that conductance decreases after a systemic response commanded by root system signals under a particular stress condition. This process leads to the closure of the stomata [107]. During crop water stress, stomatal conductance in the optical sensor system appears to be closed as leaves experience water stress, particularly when the leaf water potential decreases below a certain threshold [108].

6. Thermometric Sensing Systems and Crop Water Stress

Remote–sensing systems (e.g., thermometric infrared and microwave) are used for a higher output of data in crop water stress assessment. This technology is involved in determining the energy reflected from source crops, whereby their temperature is analyzed, and crop water stress, evapotranspiration, and irrigation water requirements are evaluated [109]. The system analyzes energy emitted from the target crop and evaluates the actual soil moisture and crop water availability [110]. It assesses the crop water stress of large areas due to their potential to gather large datasets and is considered more efficient than other remote–sensing systems.

Thermal infrared systems are widely utilized for their efficient ability to detect crop water stress. Thermal infrared systems compare the temperatures of all target objects and provide a mean average value for the leaf temperature and foliage areas.

A thermal infrared imaging system is composed of cooled and uncooled cameras. Cooled infrared cameras determine slight temperature variations from highly sensitive data and can be used at limited spatial scales [111–113]. Uncooled infrared cameras are comparatively lighter and can be reliably utilized for a vast variety of experiments at an affordable price. They are used on the ground and in UAV systems.

These systems monitor crop water stress and assess crop water levels. Uncooled cameras, such as HSI3000 (Palmer Wahl Instruments Inc., Asheville, NC, USA), are utilized to acquire infrared thermal and microwave images from the crop and canopy source. The range of the camera is 8–14 microns. The camera is based on an imaging system known as the focal plane array (FPA) detector, which provides a high resolution of 160 × 120 pixels using a single sensor camera. This sensor provides an instantaneous field of view (IFOV) option of 1.3 mrad and a field of view (FOV) option of 20° × 15°. This feature of the sensor allows for a spatial range of 0.4 mm × 0.4 mm from a reduced range of 0.3 m. The sensor

perfectly detects objects with temperatures ranging from 23 to 25 °C, a thermal conductance sensitivity of 0.15 °C, and a temperature precision from 2 to −2 °C [114–122].

Studies on the successful utilization of thermal and microwave sensors have been conducted. Cohen et al. [123] developed a thermal sensing system for crop stress analysis. The system mapped leaf water potential under different irrigation intervals while providing promising results that were later validated by others. There are many studies considered as alternative methods for determining crop water stress using the thermal infrared imaging system for spatial variability analysis. Fuchs [124] developed leaf temperature variation analysis by using the theoretical method of the crop energy balance and reported that stress is directly linked to the crop. Jones et al. [125,126] conducted experiments using the thermal and microwave method to determine a more accurate approach for crop water stress under full and uniform cover.

Previous studies on thermal imagery analysis for crop water stress estimation provided an average and inaccurate measured temperature for wheat and maize crops. Many limitations such as the cells of dead leaves, the trunk, or soil might be comprised in sampling, which can lead to non–realistic data or major errors in the results [127]. Technological advancements have resulted in state–of–the–art systems for determining precise crop water stress using thermal imagery systems with suitable spatial analysis of the soil surface. Thermal sensors integrated with near–infrared (NIR) and visible sensors exclude the non–leaf products from all samples and determine the canopy temperature with the option of choosing various parts of the leaf and canopy for crop water stress analysis [128].

Studies found that, despite the latest developments in the infrared thermal system, the hardware and software still need to be significantly improved using advanced knowledge to analyze leaf and canopy temperatures and crop water stress with precise soil–based measurements. Data on these factors need to be developed in order to interpret crop water stress estimation in a more accurate way [129]. A thermal infrared system is used to determine vegetation water content. The system analyzes imagery data and estimates crop water capacity and water stress [130,131]. This analysis is of significant importance and can be used to make better decisions in a more timely manner.

7. Land Surface Temperature Sensing Systems and Crop Water Stress

Land surface temperature (LST) is the main factor in modern agriculture that is used to analyze crop water stress using remote–sensing systems [132]. Many studies have been performed to validate the LST system for irrigation mapping [133], crop observation, evapotranspiration, and crop water stress monitoring [134].

Nugraha et al. [135] tested a multi–scale imagery system for conducting a crop water stress analysis. The study showed that the identified crop water stress using the LST method provided a linear trend with the other available data. The LST accuracy was recorded as 1 °C. Another study showed that the water deficit index (WDI) based on imagery sensing data could precisely determine crop water stress. The acquired imagery data provided an indicator to analyze the normalized green–red difference index (NGRDI), while the WDI recorded a spatial resolution value of 0.25 m [136].

In the LST method, the system uses two types of pixels for evaluating crop water stress: Cold and hot. The cold pixel system is able to acquire data from the crop with no crop water stress, while the hot pixel system acquires data from the water–stressed crop. Evapotranspiration processes were recorded with the help of the surface energy balance using remote sensing of hot and cold pixels [134]. The study provided recommendations for the use of the cold pixel system and suggested that, with minute changes in the hot pixel system, significant results can be achieved. For regions (particularly arid regions) with high crop water stress, the hot pixel system is utilized to determine precise crop water stress content [137].

The hot pixel system is in significant demand for evaluating LST (°C), as it is directly linked to crop water stress. Accurate LST determination depends on the precise measurement of soil surface emissivity, which is considered a dynamic function due to abrupt

variations in land cover, plant growth, and other stress conditions. The inclusion of a soil emissivity analysis results in a considerable overestimation of LST. However, if emission is overestimated, the determination based on LST will be inaccurate.

Dhungel et al. [138] argued that when evaluating crop water stress, LST plays a significant role in providing the required parameters, such as evapotranspiration and water and surface energy balances. The data for the required parameters are acquired from the source target using the thermal infrared satellite system. This technical process includes multiple functions for atmospheric corrections, radiometric analysis, emissivity management, and cloud removal, which are complex methods and require several other parameters to be involved.

A study conducted by Heinemann et al. [139] for retrieving LST, including climatological emissions and atmospheric management, revealed a value of 0.157 (standard deviation, SD = 0.227), while the full vegetation revealed a value of 0.905 (SD = 0.111) by means of four rape plots (healthy varieties). LST values showed a maximum deviation (dLST) of 1.0 K for varieties and bare soil surfaces. An accurate environmental temperature is widely adapted to measure crop water stress [140]. Malbéteau et al. [141] found an LST mean of 0.99, while the root mean square error (RMSE) was 0.68 °C, acquired using the UAV system for crop water stress assessment. The grass surface showed an RMSE value of 0.45 °C. Torres–Rua et al. [142] analyzed spectral functions to obtain thermal emissivity patterns. That study suggested that certain characteristics, such as emissivity values ranging from 0.99 to 0.96, can be used to accurately estimate crop water stress.

8. Multispectral Sensing Systems and Crop Water Stress

Figure 5 shows the A–type optical multispectral sensing system, which is composed of a prism, sensor, crating, and lens. The camera system captures the external light striking at the prism, which breaks the light into its minor proportions. Ultimately, the sensor creates multispectral imagery data. Meanwhile, the C–type filter is composed of multiple spectral filters. The filter acquires crop imagery data, in the minimum processing time, to provide multi–layer imagery information. Multispectral UAV remote–sensing systems are equipped with high–resolution pixel cameras that precisely analyze crop water stress. They are available at lower costs, which makes them more accessible, cheap, and effective trackers of crop water stress. The camera system simultaneously displays three color bands, red, green, and blue, with natural color imagery. The AIRPHEN multispectral camera provides reliable crop water stress results using a lens with an 8 mm focal length; the lens acquires images of 1280 × 960 pixels, which can be saved in various formats. The AIRPHEN camera system is constructed with six other separate camera systems that have a filter corresponding to 450, 530, 560, 675, 730, and 850 nm wavelengths and provides a spectral resolution of 10 nm in different conditions. The combination intervals of the separate cameras are adjusted intelligently such that the dynamics and saturation are maximized. The camera system acquires imagery data on a continuous basis at a 1 Hz frequency wavelength [143].

Various studies, e.g., by Gago et al. [45], have reported a detailed analysis on drought and moisture values for crop water stress assessment. This information is acquired by remote sensors to obtain electromagnetic–range reflectance data. It is feasible that the light spectra of crops are variable and change with each crop type, tissue water levels, and intrinsic parameters. A previous study used the backscattering (dB) C–band data extracted from the multispectral system. For Sentinel–1, Landsat–8, and combination methods, significant results related to RMSE were recorded, such as 0.89, 0.24, and 0.31 (mm day–1), respectively [144]. The crop reflectance at a particular electromagnetic wavelength is analyzed according to the morphological and chemical features of the source surface. Crop water stress analysis is performed on the given wavelength spectra: (i) Ultraviolet wavelength (UV) spectra ranging from 10 to 380 nm; (ii) visible wavelength spectra in the blue range (450–495 nm), the green range (495−570 nm), and the red range (620–750 nm); and (iii) near–infrared wavelength spectra (850–1700 nm) [145].

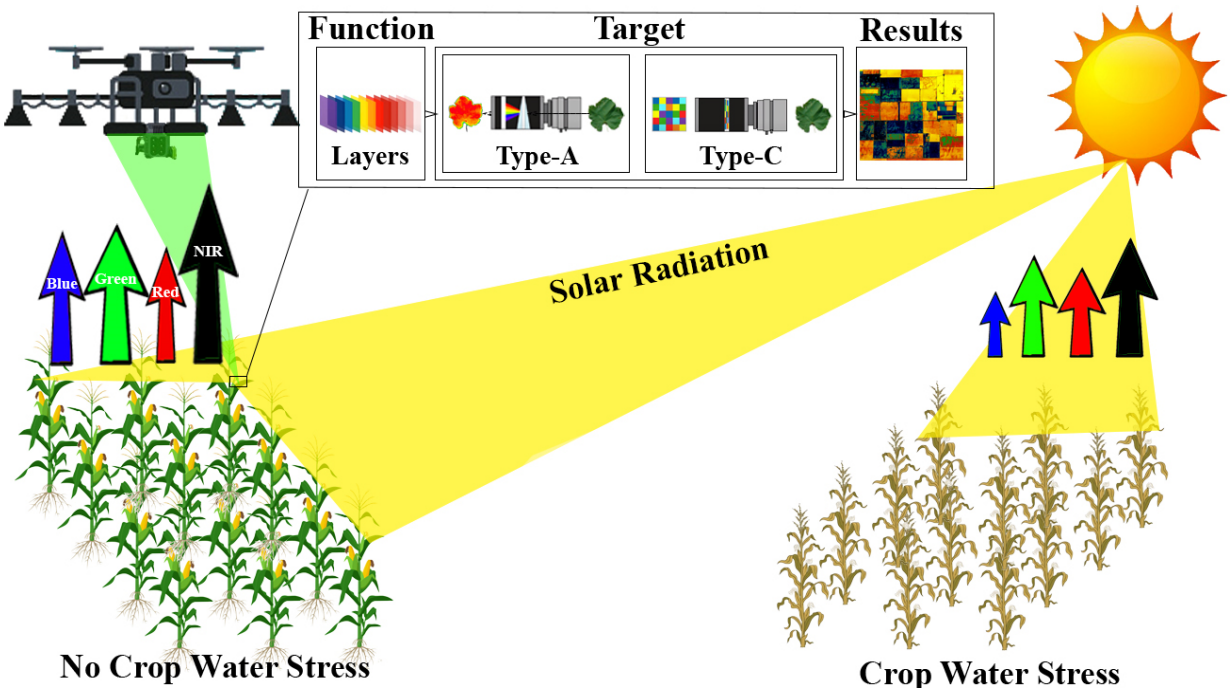

Figure 5. Crop water stress estimation using the multispectral remote–sensing system.

8.1. Spaceborne Multispectral Sensing Systems

In 1967, the medium–resolution spaceborne system acquired wide multispectral imagery data to study crop water stress. The Landsat program is considered to be an initial source of multispectral data analysis for crop water stress [146,147]. Secondly, the French mid–resolution high–quality multispectral system provides crop water stress assessment on a regular basis. The imagery dataset is commercially available but is considerably more expensive than Landsat, while the stereo groups are assembled with special tools. Okujeni et al. [148] report advanced spaceborne imaging spectroscopy that delivers more discriminate analysis by comparing contemporary imagery datasets. Separating the spectral temporal metrics (STMs) data of the acquired Landsat imagery provides the benefit of complete crop water stress temporal information [149]. Thirdly, the GeoEye system (OrbView and IKONOS) and digital globe system (WorldView and QuickBird) acquire multispectral high–resolution data for the determination of crop water stress. The dataset of this system is commercially available with specified parameters and at a cheaper price. Ibrahim et al. [150] tested the multispectral sensor, which includes the spatial and spectral resampling of crop water stress that belongs to the spaceborne multispectral system. The study analyzed resampled crop water stress imagery and showed that the spaceborne multispectral sensor has the capacity for sediment classification. A study assessed the interoperability of the SPOT–5 Take–5 data for crop parameter (basal crop coefficient (Kcb) values and the length of the crop's development stages) retrieval and crop type classification, with a focus on crop water requirements. A high R^2 correlation between NDVI and backscatter analysis was recorded for crops, showing that optical data can be replaced by microwave data in the availability of cloud cover. However, proper identification of each stage of the crop cycle was missing due to the lack of earth–observation data [151].

8.2. Airborne Multispectral Sensing Systems

A computerized aerial camera system was initially developed to improve the potential of the film camera system. The airborne multispectral system provides commercially available large– and medium–scale analysis that is based on color–infrared, natural color, and panchromatic imagery for the determination of crop water stress. This is currently considered the most reliable multispectral remote–sensing equipment [152]. Studies show

that novel airborne multispectral systems that were initiated have become operational for crop water stress assessments, including the Optech Titan mission, which provided data for wavelengths from 532 to 1550 nm. The other airborne multispectral system, known as Riegl VQ–1560i–DW, provides data for the wavelength range 532–1064 nm. The color band differentiates the magnitude of absorbed light. These differences are analyzed on the basis of land cover characteristics [153]. The Optech Titan system analysis presents crop water stress using spectral [154], texture [155], and geometrical parameters [156]. The airborne multispectral analysis provides high–accuracy characterization of the dominant source class [157]. Studies validating the application of the Optech Titan system for crop water stress characterization based on intensity and structural parameters have provided significant results [158].

9. Hyperspectral Sensing Systems and Crop Water Stress

Figure 6 shows the process of data acquisition by first observing the target with the help of a hyperspectral camera and then delivering a large amount of data to a user. The hyperspectral camera system is based on the continuous acquisition of spectral analysis. The system provides a correlation between crop health and spectral characteristics [159]. Its objective is to detect crop reactions under environmental conditions and provide an estimation of crop water stress in an easy and reliable way. The wavelength band of the hyperspectral remote–sensing approach ranges from 8 to 14 μm [160]. Atmospheric correction, emissivity, and temperature separation methods need to be applied for hyperspectral crop water stress determination [161]. For atmospheric correction, the spectral radiance analysis, performed by the system, is composed of the source radiance emission and emission radiated by the surroundings that are reflected from the surface of the source. Further impacts on the system are created by scattering radiation, absorption, and emission. Studies have ignored many parameters from the empirical forms of measurement, but it was later found via the MIDAC FTIR spectrometer system that these data and results are comprised of ineffective variables that impacted the results [162]. This was later updated with the required parameters. For emissivity and temperature separation, the data and information need to be known. The determined spectral radiance in the emissivity separation is the parameter of the spectral emissive and acquired environmental temperature of the source target. Therefore, it needs to be considered that radiance is evaluated in the n–band wavelength, which is correlated with both the soil temperature and emissivity parameters, which need to be known to analyze the surface temperatures using the hyperspectral remote–sensing system for crop water stress analysis [163].

Hyperspectral remote sensing for crop water stress has, so far, been rarely studied due to the lack of attention from researchers, which occurred for various reasons. Ribeiro da Luz et al. [164] reports that crop plants provide non–suitable spectral parameters when acquired by the hyperspectral system because of the following: (i) The high cost of the hyperspectral systems, which makes them inaccessible to many, (ii) the low and minor spectral emissivity acquired by the system related to crop water stress, which provides non–significant data, and (iii) there is less chance of detecting minor crop changes such as growth and development. Studies show that the particular spectral characteristics are relevant to different crop types [165–167]. Tests on defining the correlation between biochemical stress effects and leaf structural characteristics are reported by Buitrago et al. [168] and Buitrago Acevedo et al. [169].

Further studies are required to develop and upgrade the hyperspectral remote–sensing applications. The traditional system is unable to provide effective and precise data with the current package of system applications. Our study proposes that there is a serious need to develop mathematical algorithms that are flexible, reliable, and cheap and that yield effective results in all environments. The system also lacks satellite mission designs, including a Landsat surface temperature monitor (LSTM) [170–173], a hyperspectral infrared image (HyspIRI) [174–179], and a high–resolution temperature and spectral emission mapper (HiTeSEM) [180–184], which are able to acquire crop water stress on a global

scale [185–189]. A previous study proposed three new spectral absorption indices, the results of which estimated a suitable correlation for the equivalent water thickness compared to the fuel moisture content; however, the third index outperformed other indices at the leaf level [190].

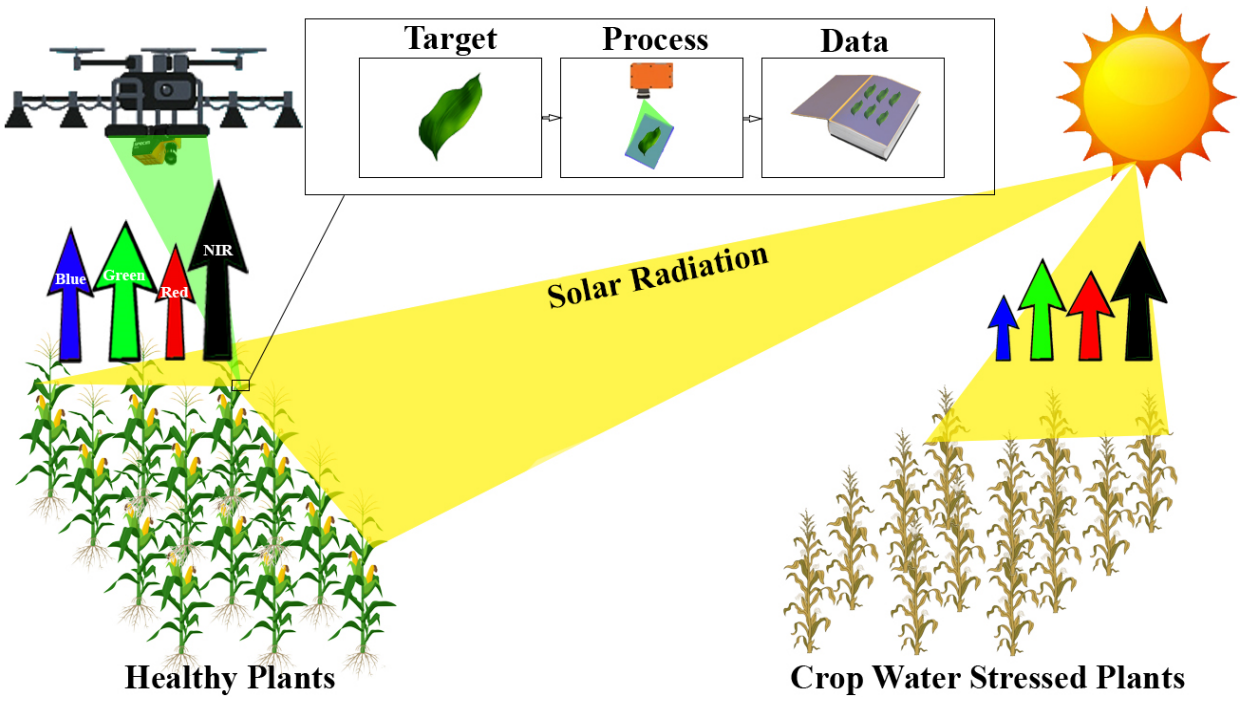

Figure 6. Remote–sensing hyperspectral camera system is used to analyze crop water stress (in both healthy and stressed plants), identify gaps in crop production, and provide suggestions to mitigate with stress conditions.

10. LiDAR Sensing System and Crop Water Stress

Light detection and ranging (LiDAR) can be understood to be a dynamic remote–sensing system that delivers accurate 3D data by analyzing the flight time of the released laser light from the sensor to the source. The directed short–band laser light efficiently infiltrates the crop canopy and is less affected by the infiltrated light [191]. Because of this, it possesses a great capacity for field–based crop water stress estimation [192]. The LiDAR system is an emerging system for the analysis of field crop water stress. Currently, research is being conducted on advancing algorithms to intelligently extract crop water stress from LiDAR information. For example, Jin et al. [193] recommended techniques that combine algorithms with geometric regulations to precisely deliver crop water stress and their relationship with crop parameters using LiDAR analysis. The LiDAR system was tested to measure leaf water stress in different crops, which revealed a strong relationship between leaf water stress and the number of points acquired using LiDAR [194]. These research experiments concretely validated that the LiDAR system is perfect for analyzing crop water stress in a non–destructive way. New methods of analyzing phenotypic characteristics for crop water stress using the LiDAR system are in progress [195]. LiDAR, used in an integrative method with other sensing systems, delivers new insights on crop water stress that can be established by the spectral reflective method and the required crop characteristics. Likewise, the LiDAR system estimates aboveground biomass and canopy as part of a crop water stress platform, offering analysis of the high correlation of volume and aboveground biomass and providing vertical measurements of crop biochemical characteristics using the HIS LiDAR technique [196].

Roth et al. [197] studied the heat maps (plot a) of the leaf area index (LAI) (m^2 m^{-2}) and mean leaf angle (°) (plot b). The cumulative distribution function (cdf) for the leaf angle distribution (LAD) (°) was also estimated using a cumulative sum at the normalized

histogram data (plot c). The study determined the cdf for each of the corresponding pixels during the tests. The planophile and spherical distributions are analyzed as a comparison to the disseminations that were utilized for the 10 m vegetation cover.

The estimation of the LiDAR system to crop water stress is less developed, while allowing the depths and types of data delivered by the LiDAR system in a short period of time at a lower cost, specifically in relation to crop water stress [198]. This study evidenced the inherent faults in the procedure, vulnerability, and inefficiency in acquiring physiological traits and incomplete crop water stress representation. The aforementioned factors suggest that, in crop water stress, the LiDAR system will need to be linked with another system to address the above–stated drawbacks. However, further studies are required to conduct the exploration of crop responses to crop water stress using LiDAR systems. The reliability of LiDAR in analyzing crop water stress and how crops respond to water stress conditions still need to be explored.

11. Future Directions

Remote–sensing systems can clearly be applied in target water stress identification. Other than applications such as crop growth assessment, irrigation, and crop losses, digital image techniques are performed for leaf and canopy phenotypic classification to detect crop water stress with the help of digital imagery data. The latest approaches to remote sensing for digital imagery used for crop water stress estimation have delivered significant results. The research mostly showed crop water stress at three stages: No water stress (optimum moisture), medium water stress (light drought stress), and high water stress (drought stress). These techniques delivered promising results for the estimation of crop water stress, with precision from 83–99% [199–201]. Visible imagery techniques of crop canopies and leaves show a diverse set of phenotypes under water–stressed conditions. Analyzing crop water stress variation is difficult and costly with manual and test–site sensors because (i) data acquisition with manual sensors is laborious and (ii) the price of sensors is high. Efficient ground–based sensors and UAV systems are becoming important to advance image collection. Different symptoms are important to immediately estimate crop water stress, which cannot be estimated by only using a visible image system, yet spectral bands (infrared, thermal, and multispectral) have not been fully exploited. Considering this, these methods could be performed in an integrative fashion for estimating crop water stress in drought conditions. The SMAP technique (L–band) is highly effective for determining soil moisture, as it gives flexible parameters that are utilized in cold as well as hot regions, and it is used by NASA and ISRA. Moreover, the FLEX system is highly compatible and will be used by ISRA to analyze SIF and reflectance for its 2023 missions, followed by SEBAL for leaf and canopy thermal imagery (Table 2). Findings from studies related to the detection of crop water stress using remote–sensing systems will further upgrade the scope of remote–sensing technology, management, and techniques and open up new perspectives for research on crop water stress management.

Machine learning is important for improving system efficiency and quality. For example, a microcontroller–based signal processor (MSP430) supports soil and environmental sensors for the proper assessment of crop water stress. A standalone wireless sensor system, composed of a gateway and wireless sensory nodes, is a reliable source for analyzing crop water and soil moisture stress factors as presented in Table 2. Machine–learning–based artificial neural networks (ANNs) forecast an accurate level of crop water stress. An ANN obtains the data using a wireless sensory network supported by infrared thermometers (IRTs) that are attached to calculate the irrigation levels. Ultimately, the system acquires data from the crop, soil, and environmental factors, transmits it to a computerized irrigation–controlled algorithm, and provides crop, soil, and environmental stress analysis. Another machine–learning system, the ARS–pivot (ARSP) system, simplifies the ANN analysis and reliably predicts the potential crop water stress by analyzing previous data related to IRTs. ANN–based machine–learning systems show promise for the efficient forecast analysis of crop water stress [202]. Thus, the development of ANN and ARS

systems can potentially provide beneficial aspects in forecasting crop water stress. This can also help in generating future data, even in particular conditions where the direct analysis of crop water stress is not possible due to bad visibility, non–availability, or high cost of the system.

Table 2. Summarizing a few remote–sensing systems and presenting relevant parameters.

Remote Sensing System/Features	Advantages	Disadvantages	Temporal Resolution	Spatial Resolution	References
Thermal Sensor	High accuracy and precision; Automatic selection of the canopy	Limited commercial production	1–16 days	30 m–1 km	[203]
Optical Sensor	Multiple light sources are captured in a single image; Cost effective; Wide adoption	Limited data transmission	12 days	10–30 m	[204]
Soil Moisture Sensor	Large field coverage	Expensive	2–3 days	20–40 km	[205]

12. Conclusions

Remote–sensing technology is booming and undergoing continuous development regarding its reliability, remote functions, and efficiency. Crop water stress assessment is a technical and very complex procedure in itself and conducting these processes without remote–sensing technology is difficult. Complete field sensing using remote–sensing systems is highly appealing. Our critical review presents a modern and updated analysis of the suitability of highly advanced and modern remote–sensing systems. Our study recommends novel techniques that integrate farmers, researchers, and tech–developers so as to upgrade innovative methods with minimum cost, e.g., multispectral/hyperspectral and thermal sensing systems based on remote–sensing features. This review proposes remote–sensing systems and paves the way to designing new facilities that analyze a system's efficiencies under various environmental conditions. It demonstrates their working abilities and thus contributes to assessments of crop water stress. It further demonstrates how these technologies work together in a combined and connected setup to maximize system efficiency and minimize water deficit conditions. We have updated the literature and conducted a critical analysis in relation to simple methods for determining crop water stress factors, including crop water stress detection calculations. Due to a large number of studies on crop water stress and remote–sensing applications, there is a high number of established techniques and frameworks that are accurate, reproducible, and applicable under a wide variety of climatic, soil, and crop conditions. Future upgrades that further maximize water use efficiency and high yield production will be needed to avoid challenging conditions in the long run.

13. Patents

The graphical abstract (Figure 1) exclusively presents a new concept related to remote–sensing technology, which shows how crop water stress is detected and forecasted using crop statistics and computer software.

The concept (Figure 2) presents two different crop conditions during the crop water stress using a graphical presentation: a) normal stomatal conductance with no stress and b) a comparison of irrigation water resources and micro–environmental conditions near the plant source.

Figure 3 shows remote-sensing estimation of the crop water stress using leaf transpiration, temperature, cooling, and heating effects, and a comparison with the air and soil moisture for the potential crop water stress estimation.

Figure 5 shows the A- and C-type optical multispectral camera system and how it assesses crop water stress using different approaches.

Figure 6, as a graphical method, presents the remote-sensing hyperspectral camera system to estimate crop water stress in normal and water-stressed conditions, and shows how to address the water stress conditions.

Author Contributions: Conceptualization, U.A. and S.M.; methodology, U.A. and S.M.; software, U.A.; validation, U.A. and S.M.; formal analysis, U.A.; investigation, U.A. and S.M.; resources, U.A. and S.M.; data curation, U.A.; writing—original draft preparation, U.A. and S.M.; writing—review and editing, U.A. and S.M.; visualization, U.A. and S.M.; supervision, A.A. and S.M. All authors have read and agreed to the published version of the manuscript.

Funding: There was no funding received for the study.

Institutional Review Board Statement: Not applicable.

Informed Consent Statement: Not applicable.

Data Availability Statement: Not applicable.

Conflicts of Interest: The authors declare no conflict of interest.

References

1. FAO. *Water for Sustainable Food and Agriculture A report Produced for the G20 Presidency of Germany*; Food and Agriculture Organization of the United Nations: Rome, Italy, 2017; pp. 1–27. Available online: http://www.fao.org/3/i7959e/i7959e.pdf (accessed on 3 June 2021).
2. Chang, Y.N.; Zhu, C.; Jiang, J.; Zhang, H.; Zhu, J.K.; Duan, C.G. Epigenetic regulation in plant abiotic stress responses. *J. Integr. Plant Biol.* **2020**, *62*, 563–580. [CrossRef] [PubMed]
3. Goldstein, A.; Fink, L.; Meitin, A.; Bohadana, S.; Lutenberg, O.; Ravid, G. Applying machine learning on sensor data for irrigation recommendations: Revealing the agronomist's tacit knowledge. *Precis. Agric.* **2017**, *19*, 421–444. [CrossRef]
4. Aasen, H.; Honkavaara, E.; Lucieer, A.; Zarco-Tejada, P. Quantitative Remote Sensing at Ultra-High Resolution with UAV Spectroscopy: A Review of Sensor Technology, Measurement Procedures, and Data Correction Workflows. *Remote Sens.* **2018**, *10*, 1091. [CrossRef]
5. Tian, H.; Wang, T.; Liu, Y.; Qiao, X.; Li, Y. Computer vision technology in agricultural automation—A review. *Inf. Process. Agric.* **2020**, *7*, 1–19. [CrossRef]
6. Ali, I.; Greifeneder, F.; Stamenkovic, J.; Neumann, M.; Notarnicola, C. Review of Machine Learning Approaches for Biomass and Soil Moisture Retrievals from Remote Sensing Data. *Remote Sens.* **2015**, *7*, 16398–16421. [CrossRef]
7. Sishodia, R.P.; Ray, R.L.; Singh, S.K. Applications of Remote Sensing in Precision Agriculture: A Review. *Remote Sens.* **2020**, *12*, 3136. [CrossRef]
8. Long, D.S.; Engel, R.E.; Siemens, M.C. Measuring Grain Protein Concentration with In-line Near Infrared Reflectance Spectroscopy. *Agron. J.* **2008**, *100*, 247. [CrossRef]
9. Zhou, Z.; Majeed, Y.; Diverres Naranjo, G.; Gambacorta, E.M.T. Assessment for crop water stress with infrared thermal imagery in precision agriculture: A review and future prospects for deep learning applications. *Comput. Electron. Agric.* **2021**, *182*, 106019. [CrossRef]
10. Idso, S.B.; Jackson, R.D.; Pinter, P.J.; Reginato, R.J.; Hatfield, J.L. Normalizing the stress-degree-day parameter for environmental variability. *Agric. Meteorol.* **1981**, *24*, 45–55. [CrossRef]
11. Ru, C.; Hu, X.; Wang, W.; Ran, H.; Song, T.; Guo, Y. Evaluation of the Crop Water Stress Index as an Indicator for the Diagnosis of Grapevine Water Deficiency in Greenhouses. *Horticulturae* **2020**, *6*, 86. [CrossRef]
12. Jackson, R.D.; Idso, S.B.; Reginato, R.J.; Pinter, P.J. Canopy temperature as a crop water stress indicator. *Water Resour. Res.* **1981**, *17*, 1133–1138. [CrossRef]
13. Khorsand, A.; Rezaverdinejad, V.; Asgarzadeh, H.; Majnooni-Heris, A.; Rahimi, A.; Besharat, S.; Sadraddini, A.A. Linking plant and soil indices for water stress management in black gram. *Sci. Rep.* **2021**, *11*, 869. [CrossRef] [PubMed]
14. Inoue, Y.; Morinaga, S.; Shibayama, M. Non-destructive Estimation of Water Status of Intact Crop Leaves Based on Spectral Reflectance Measurements. *Jpn. J. Crop Sci.* **1993**, *62*, 462–469. [CrossRef]
15. Sridhar, B.B.M.; Vincent, R.K.; Roberts, S.J.; Czajkowski, K. Remote sensing of soybean stress as an indicator of chemical concentration of biosolid amended surface soils. *Int. J. Appl. Earth Obs. Geoinf.* **2011**, *13*, 676–681. [CrossRef]
16. Yi, Q.-xiang; Bao, A.-ming; Wang, Q.; Zhao, J. Estimation of leaf water content in cotton by means of hyperspectral indices. *Comput. Electron. Agric.* **2013**, *90*, 144–151. [CrossRef]

17. Carter, G.A. Responses of Leaf Spectral Reflectance to Plant Stress. *Am. J. Bot.* **1993**, *80*, 239. [CrossRef]
18. Peñuelas, J.; Filella, I.; Biel, C.; Serrano, L.; Savé, R. The reflectance at the 950–970 nm region as an indicator of plant water status. *Int. J. Remote Sens.* **1993**, *14*, 1887–1905. [CrossRef]
19. Peñuelas, J.; Gamon, J.A.; Fredeen, A.L.; Merino, J.; Field, C.B. Reflectance indices associated with physiological changes in nitrogen- and water-limited sunflower leaves. *Remote Sens. Environ.* **1994**, *48*, 135–146. [CrossRef]
20. Stimson, H.C.; Breshears, D.D.; Ustin, S.L.; Kefauver, S.C. Spectral sensing of foliar water conditions in two co-occurring conifer species: Pinus edulis and Juniperus monosperma. *Remote Sens. Environ.* **2005**, *96*, 108–118. [CrossRef]
21. Zhang, L.; Zhou, Z.; Zhang, G.; Meng, Y.; Chen, B.; Wang, Y. Monitoring the leaf water content and specific leaf weight of cotton (Gossypium hirsutum L.) in saline soil using leaf spectral reflectance. *Eur. J. Agron.* **2012**, *41*, 103–117. [CrossRef]
22. Yi, Q.; Wang, F.; Bao, A.; Jiapaer, G. Leaf and canopy water content estimation in cotton using hyperspectral indices and radiative transfer models. *Int. J. Appl. Earth Obs. Geoinf.* **2014**, *33*, 67–75. [CrossRef]
23. Cohen, W.B. Temporal versus spatial variation in leaf reflectance under changing water stress conditions. *Int. J. Remote Sens.* **1991**, *12*, 1865–1876. [CrossRef]
24. Mirzaie, M.; Darvishzadeh, R.; Shakiba, A.; Matkan, A.A.; Atzberger, C.; Skidmore, A. Comparative analysis of different uni- and multi-variate methods for estimation of vegetation water content using hyper-spectral measurements. *Int. J. Appl. Earth Obs. Geoinf.* **2014**, *26*, 1–11. [CrossRef]
25. Holzman, M.E.; Rivas, R.E.; Bayala, M.I. Relationship between TIR and NIR-SWIR as Indicator of Vegetation Water Availability. *Remote Sens.* **2021**, *13*, 3371. [CrossRef]
26. Qi, Y.; Dennison, P.E.; Jolly, W.M.; Kropp, R.C.; Brewer, S.C. Spectroscopic analysis of seasonal changes in live fuel moisture content and leaf dry mass. *Remote Sens. Environ.* **2014**, *150*, 198–206. [CrossRef]
27. Danson, F.M.; Steven, M.D.; Malthus, T.J.; Clark, J.A. High-spectral resolution data for determining leaf water content. *Int. J. Remote Sens.* **1992**, *13*, 461–470. [CrossRef]
28. Podder, A.K.; Bukhari, A.A.; Islam, S.; Mia, S.; Mohammed, M.A.; Kumar, N.M.; Cengiz, K.; Abdulkareem, K.H. IoT based smart agrotech system for verification of Urban farming parameters. *Microprocess. Microsyst.* **2021**, *82*, 104025. [CrossRef]
29. de Jong, S.M.; Addink, E.A.; Doelman, J.C. Detecting leaf-water content in Mediterranean trees using high-resolution spectrometry. *Int. J. Appl. Earth Obs. Geoinf.* **2014**, *27*, 128–136. [CrossRef]
30. Bowyer, P.; Danson, F.M. Sensitivity of spectral reflectance to variation in live fuel moisture content at leaf and canopy level. *Remote Sens. Environ.* **2004**, *92*, 297–308. [CrossRef]
31. Ceccato, P.; Flasse, S.; Tarantola, S.; Jacquemoud, S.; Grégoire, J.-M. Detecting vegetation leaf water content using reflectance in the optical domain. *Remote Sens. Environ.* **2001**, *77*, 22–33. [CrossRef]
32. Wang, J.; Xu, R.; Yang, S. Estimation of plant water content by spectral absorption features centered at 1450 nm and 1940 nm regions. *Environ. Monit. Assess.* **2008**, *157*, 459–469. [CrossRef] [PubMed]
33. Zhang, J.H.; Xu, Y.; Yao, F.M.; Wang, P.J.; Guo, W.J.; Li, L.; Yang, L.M. Advances in estimation methods of vegetation water content based on optical remote sensing techniques. *Sci. China Technol. Sci.* **2010**, *53*, 1159–1167. [CrossRef]
34. Reginato, R.J. Field quantification of crop water stress. *Trans. Am. Soc. Agric. Eng.* **1983**, *26*, 0772–0775. [CrossRef]
35. Idso, S.B. Non-water-stressed baselines: A key to measuring and interpreting plant water stress. *Agric. Meteorol.* **1982**, *27*, 59–70. [CrossRef]
36. Jackson, R.D.; Reginto, R.J.; Idso, S.B. Wheat canopy temperature: A practical tool for evaluating water requirements. *Water Resour. Res.* **1977**, *13*, 51–656. [CrossRef]
37. Nanda, M.K.; Giri, U.; Bera, N. Canopy Temperature-Based Water Stress Indices: Potential and Limitations. In *Advances in Crop Environment Interaction*; Bal, S., Mukherjee, J., Choudhury, B., Dhawan, A., Eds.; Springer: Singapore, 2018. [CrossRef]
38. Tanner, C.B. Plant Temperatures 1. *Agron. J.* **1963**, *55*, 210–211. [CrossRef]
39. Monteith, J.L.; Szeicz, G. Radiative temperature in the heat balance of natural surfaces. *R. Meteorol. Soc.* **1962**, *88*, 496–507. [CrossRef]
40. Maes, W.H.; Steppe, K. Estimating evapotranspiration and drought stress with ground-based thermal remote sensing in agriculture: A review. *J. Exp. Bot.* **2012**, *63*, 4671–4712. [CrossRef]
41. Bian, J.; Zhang, Z.; Chen, J.; Chen, H.; Cui, C.; Li, X.; Chen, S.; Fu, Q. Simplified evaluation of cotton water stress using high resolution unmanned aerial vehicle thermal imagery. *Remote Sens.* **2019**, *11*, 267. [CrossRef]
42. Pou, A.; Diago, M.P.; Medrano, H.; Baluja, J.; Tardaguila, J. Validation of thermal indices for water status identification in grapevine. *Agric. Water Manag.* **2014**, *134*, 60–72. [CrossRef]
43. Crawford, K.E. *Remote Sensing of Almond and Walnut Tree Canopy Temperatures Using an Inexpensive Infrared Sensor on A Small Unmanned Aerial Vehicle*; University of California Davis: Davis, CA, USA, 2012.
44. Sepúlveda-Reyes, D.; Ingram, B.; Bardeen, M.; Zúñiga, M.; Ortega-Farías, S.; Poblete-Echeverría, C. Selecting canopy zones and thresholding approaches to assess grapevine water status by using aerial and ground-based thermal imaging. *Remote Sens.* **2016**, *8*, 822. [CrossRef]
45. Gago, J.; Douthe, C.; Coopman, R.E.; Gallego, P.P.; Ribas-Carbo, M.; Flexas, J.; Escalona, J.; Medrano, H. UAVs challenge to assess water stress for sustainable agriculture. *Agric. Water Manag.* **2015**, *153*, 9–19. [CrossRef]
46. Sepulcre-Cantó, G.; Zarco-Tejada, P.J.; Jiménez-Muñoz, J.C.; Sobrino, J.A.; de Miguel, E.; Villalobos, F.J. Detection of water stress in an olive orchard with thermal remote sensing imagery. *Agric. For. Meteorol.* **2006**, *136*, 31–44. [CrossRef]

47. Egea, G.; Padilla-Díaz, C.M.; Martinez-Guanter, J.; Fernández, J.E.; Pérez-Ruiz, M. Assessing a crop water stress index derived from aerial thermal imaging and infrared thermometry in super-high density olive orchards. *Agric. Water Manag.* **2017**, *187*, 210–221. [CrossRef]
48. Mohanty, B.P.; Cosh, M.H.; Lakshmi, V.; Montzka, C. Soil Moisture Remote Sensing: State-of-the-Science. *Vadose Zone J.* **2017**, *16*, 1–9. [CrossRef]
49. Entekhabi, D.; Yueh, S.; O'Neill, P.E.; Kellogg, K.; Allen, A.; Bindlish, R. *SMAP Handbook–Soil Moisture Active Passive: Mapping Soil Moisture and Freeze/Thaw from Space*; Publ. JPL 2014, 400-1567; NASA, Jet Propulsion Lab: Pasadena, CA, USA, 2014. Available online: https://limo.libis.be/primo-explore/fulldisplay?docid=LIRIAS1741023&context=L&vid=Lirias&search_scope=Lirias&tab=default_tab&lang=en_US&fromSitemap=1 (accessed on 16 July 2021).
50. Gruber, A.; Su, C.H.; Zwieback, S.; Crowd, W.; Dorigo, W.; Wagner, W. Recent advances in (soil moisture) triple collocation analysis. *Int. J. Appl. Earth Obs. Geoinf.* **2016**, *45*, 200–211. [CrossRef]
51. Paloscia, S.; Pettinato, S.; Santi, E.; Notarnicola, C.; Pasolli, L.; Reppucci, A. Soil moisture mapping using Sentinel-1 images: Algorithm and preliminary validation. *Remote Sens. Environ.* **2013**, *134*, 234–248. [CrossRef]
52. Hornacek, M.; Wagner, W.; Sabel, D.; Truong, H.L.; Snoeij, P.; Hahmann, T. Potential for high resolution systematic global surface soil moisture retrieval via change detection using Sentinel-1. *IEEE J. Sel. Top. Appl. Earth Obs. Remote Sens.* **2012**, *5*, 1303–1311. [CrossRef]
53. Moreira, A.; Krieger, G.; Hajnsek, I.; Papathanassiou, K.; Younis, M.; Lopez-Dekker, P. Tandem-L: A highly innovative bistatic SAR mission for global observation of dynamic processes on the Earth's surface. *IEEE Geosci. Remote Sens. Mag.* **2015**, *3*, 8–23. [CrossRef]
54. Bogena, H.R.; Huisman, J.A.; Güntner, A.; Hübner, C.; Kusche, J.; Jonard, F. Emerging methods for noninvasive sensing of soil moisture dynamics from field to catchment scale: A review. *Water* **2015**, *2*, 635–647. [CrossRef]
55. Thibeault, M.; Cáceres, J.M.; Dadamia, D.; Soldano, A.G.; Quirno, M. Spatial and temporal analysis of the Monte Buey SAOCOM and SMAP core site. In *2015 IEEE International Geoscience and Remote Sensing Symposium (IGARSS)*; IEEE: New York, NY, USA, 2015; pp. 969–971. [CrossRef]
56. Kaihotsu, I.; Asanuma, J.; Aida, K. Evaluation of the AMSR2 L2 soil moisture product of JAXA on the Mongolian Plateau over seven years (2012–2018). *SN Appl. Sci.* **2019**, *1*, 1477. [CrossRef]
57. Kolassa, J.; Gentine, P.; Prigent, C.; Aires, F. Soil moisture retrieval from AMSR-E and ASCAT microwave observation synergy. Part 1: Satellite data analysis. *Remote Sens. Environ.* **2016**, *173*, 1–14. [CrossRef]
58. NISAR: The NASA-ISRO SAR Mission. Water: Vital for Life and Civilization. © 2019 California Institute of Technology. Government Sponsorship Acknowledged. Available online: https://nisar.jpl.nasa.gov/system/documents/files/15_NISARApplications_SoilMoisture1.pdf (accessed on 16 July 2021).
59. DLR. Tandem-L, Satellite Mission Proposal for Monitoring Dynamic Processes on the Earth's Surface. Cologne, April 2016. Reprinting or Other Use (Including Excerpts) Only Permitted after Prior Agreement with DLR. DLR.de/HR. Available online: https://www.dlr.de/content/en/downloads/publications/brochures/tandem-l-brochure_1663.pdf?__blob=publicationFile&v=11 (accessed on 16 July 2021).
60. Harm-Jan, F.B.; van der Velde, R.; Su, Z. Sentinel-1 soil moisture content and its uncertainty over sparsely vegetated fields. *J. Hydrol. X* **2020**, *9*, 100066. [CrossRef]
61. Abbaszadeh, P.; Moradkhani, H.; Gavahi, K.; Kumar, S.; Hain, C.; Zhan, X.; Duan, Q.; Peters-Lidard, C.; Karimiziarani, S. High-Resolution SMAP Satellite Soil Moisture Product: Exploring the Opportunities. *Bull. Am. Meteorol. Soc.* **2021**, *102*, 4–309. [CrossRef]
62. Allen, R.G.; Pereira, L.S.; Dirk, R.; Smith, M. *Crop Evapotranspiration: Guidelines for Computing Crop Water Requirements*; FAO—Food and Agriculture Organization of the United Nations: Rome, Italy, 1998. Available online: http://www.fao.org/3/x0490e/x0490e00.htm (accessed on 16 July 2021).
63. Zhang, K.; Kimball, J.S.; Running, S.W. A review of remote sensing based actual evapotranspiration estimation. *WIREs Water* **2016**, *3*, 834–853. [CrossRef]
64. López-López, R.; Ramón, A.R.; Cohen, I.S.; Bustamante, W.O.; González-Lauck, V. Evapotranspiration and Crop Water Stress Index in Mexican Husk Tomatoes (*Physalis ixocarpa* Brot). In *Evapotranspiration—From Measurements to Agricultural and Environmental Applications*; Giacomo Gerosa, G., Ed.; Mexico. Project: Irrigation Scheduling and Programming; IntechOpen: London, UK, 2011; p. 187.
65. Marino, S.; Ahmad, U.; Ferreira, M.I.; Alvino, A. Evaluation of the Effect of Irrigation on Biometric Growth, Physiological Response, and Essential Oil of *Mentha spicata* (L.). *Water* **2019**, *11*, 2264. [CrossRef]
66. Alghory, A.; Yazar, A. Evaluation of crop water stress index and leaf water potential for deficit irrigation management of sprinkler-irrigated wheat. *Irrig. Sci.* **2018**, *37*, 61–77. [CrossRef]
67. Sepaskhah, A.R.; Ilampour, S. Relationships between yield, crop water stress index (CWSI) and transpiration of cowpea (*Vigna sinensis* L). *Agronomie* **1996**, *16*, 269–279. [CrossRef]
68. Finch, J. Remote Sensing in Water Resources Management. The State of the Art. By W. G. M. Bastiaanssen. Colombo, Sri Lanka: International Water Management Institute pp. 118, US$25.00 (developing countries US$12.50). ISBN 92-9090-363-5. *Exp. Agric.* **2000**, *36*, 415–418. [CrossRef]

69. Bastiaanssen, W.G.; Noordman, E.J.; Pelgrum, H.; Davids, G.; Thoreson, B.P.; Allen, R.G. SEBAL Model with Remotely Sensed Data to Improve Water-Resources Management under Actual Field Conditions. *J. Irrig. Drain. Eng.* **2005**, *131*, 85–93. [CrossRef]
70. Sun, X.; Zou, C.B.; Wilcox, B.; Stebler, E. Effect of Vegetation on the Energy Balance and Evapotranspiration in Tallgrass Prairie: A Paired Study Using the Eddy-Covariance Method. *Bound. Layer Meteorol.* **2018**, *170*, 127–160. [CrossRef]
71. Shellie, K.C.; King, B.A. Application of a Daily Crop Water Stress Index to Deficit Irrigate Malbec Grapevine under Semi-Arid Conditions. *Agriculture* **2020**, *10*, 492. [CrossRef]
72. Romero-Trigueros, C.; Bayona Gambín, J.M.; Nortes Tortosa, P.A.; Alarcón Cabañero, J.J.; Nicolás Nicolás, E. Determination of Crop Water Stress Index by Infrared Thermometry in Grapefruit Trees Irrigated with Saline Reclaimed Water Combined with Deficit Irrigation. *Remote Sens.* **2019**, *11*, 757. [CrossRef]
73. Akkuzu, E.; Kaya, Ü.; Çamoğlu, G.; Mengü, G.P.; Aşik, Ş. Determination of Crop Water Stress Index and Irrigation Timing on Olive Trees Using a Handheld Infrared Thermometer. *J. Irrig. Drain. Eng.* **2013**, *139*, 728–737. [CrossRef]
74. Dauphin, L. Detecting Invisible Plant Stress Using MODIS Data from NASA EOSDIS/LANCE and GIBS/Worldview and Evaporative Stress Data from the ECOSTRESS Team. Available online: https://earthobservatory.nasa.gov/images/145823/detecting-invisible-plant-stress2019 (accessed on 3 June 2021).
75. GLEAM. (n.d.). GLEAM | Global Land Evaporation Amsterdam Model. Available online: https://www.gleam.eu/ (accessed on 4 October 2021).
76. Gerhards, M.; Schlerf, M.; Mallick, K.; Udelhoven, T. Challenges and Future Perspectives of Multi-/Hyperspectral Thermal Infrared Remote Sensing for Crop Water-Stress Detection: A Review. *Remote Sens.* **2019**, *11*, 1240. [CrossRef]
77. Nagasubramanian, K.; Jones, S.; Singh, A.K.; Sarkar, S.; Singh, A.; Ganapathysubramanian, B. Plant disease identification using explainable 3D deep learning on hyperspectral images. *Plant Methods* **2019**, *15*, 98. [CrossRef] [PubMed]
78. Chlingaryan, A.; Sukkarieh, S.; Whelan, B. Machine learning approaches for crop yield prediction and nitrogen status estimation in precision agriculture: A review. *Comput. Electron. Agric.* **2018**, *151*, 61–69. [CrossRef]
79. Camino, C.; González-Dugo, V.; Hernández, P.; Sillero, J.C.; Zarco-Tejada, P.J. Improved nitrogen retrievals with airborne-derived fluorescence and plant traits quantified from VNIR-SWIR hyperspectral imagery in the context of precision agriculture. *Int. J. Appl. Earth Obs. Geoinf.* **2018**, *70*, 105–117. [CrossRef]
80. Zarco-Tejada, P.J.; González-Dugo, M.V.; Fereres, E. Seasonal stability of chlorophyll fluorescence quantified from airborne hyperspectral imagery as an indicator of net photosynthesis in the context of precision agriculture. *Remote Sens. Environ.* **2016**, *179*, 89–103. [CrossRef]
81. Mohammed, G.H.; Colombo, R.; Middleton, E.M.; Rascher, U.; van der Tol, C.; Nedbal, L.; Goulas, Y.; Pérez-Priego, O.; Damm, A.; Meroni, M.; et al. Remote sensing of solar-induced chlorophyll fluorescence (SIF) in vegetation: 50 years of progress. *Remote Sens. Environ.* **2019**, *231*, 111177. [CrossRef] [PubMed]
82. Gautam, D.; Pagay, V. A Review of Current and Potential Applications of Remote Sensing to Study the Water Status of Horticultural Crops. *Agronomy* **2020**, *10*, 140. [CrossRef]
83. Meroni, M.; Rossini, M.; Guanter, L.; Alonso, L.; Rascher, U.; Colombo, R.; Moreno, J. Remote sensing of solar-induced chlorophyll fluorescence: Review of methods and applications. *Remote Sens. Environ.* **2009**, *113*, 2037–2051. [CrossRef]
84. Wieneke, S.; Ahrends, H.; Damm, A.; Pinto, F.; Stadler, A.; Rossini, M.; Rascher, U. Airborne based spectroscopy of red and far-red sun-induced chlorophyll fluorescence: Implications for improved estimates of gross primary productivity. *Remote Sens. Environ.* **2016**, *184*, 654–667. [CrossRef]
85. Joiner, J.; Guanter, L.; Lindstrot, R.; Voigt, M.; Vasilkov, A.P.; Middleton, E.M.; Huemmrich, K.F.; Yoshida, Y.; Frankenberg, C. Global monitoring of terrestrial chlorophyll fluorescence from moderate-spectral-resolution near-infrared satellite measurements: Methodology, simulations, and application to GOME-2. *Atmos. Meas. Tech.* **2013**, *6*, 2803–2823. [CrossRef]
86. Krause, G.H.; Weis, E. Chlorophyll Fluorescence and Photosynthesis—The Basics. *Annu. Revie Plant Physiol.* **1991**, *42*, 313–349. [CrossRef]
87. Moya, I.; Camenen, L.; Evain, S.; Goulas, Y.; Cerovic, Z.G.; Latouche, G.; Flexas, J.; Ounis, A. A new instrument for passive remote sensing 1. Measurements of sunlight-induced chlorophyll fluorescence. *Remote Sens. Environ.* **2004**, *91*, 186–197. [CrossRef]
88. Du, S.; Liu, L.; Liu, X.; Zhang, X.; Zhang, X.; Bi, Y.; Zhang, L. Retrieval of global terrestrial solar-induced chlorophyll fluorescence from TanSat satellite. *Sci. Bull.* **2018**, *63*, 1502–1512. [CrossRef]
89. Frankenberg, C.; Fisher, J.B.; Worden, J.; Badgley, G.; Saatchi, S.S.; Lee, J.E.; Toon, G.C.; Butz, A.; Jung, M.; Kuze, A.; et al. New global observations of the terrestrial carbon cycle from GOSAT: Patterns of plant fluorescence with gross primary productivity. *Geophys. Res. Lett.* **2011**, *38*. [CrossRef]
90. Frankenberg, C.; O'Dell, C.W.; Berry, J.A.; Guanter, L.; Joanna, J.; Köhler, P.; Pollock, R.; Taylor, T.E. Prospects for chlorophyll fluorescence remote sensing from the Orbiting Carbon Observatory-2. *Remote Sens. Environ.* **2014**, *147*, 1–12. [CrossRef]
91. Guanter, L.; Frankenberg, C.; Dudhia, A.; Lewis, P.E.; Gómez-Dans, J.; Kuze, A.; Suto, H.; Grainger, R.G. Retrieval and global assessment of terrestrial chlorophyll fluorescence from GOSAT space measurements. *Remote Sens. Environ.* **2012**, *121*, 236–251. [CrossRef]
92. Drusch, M.; Moreno, J.; del Bello, U.; Franco, R.; Goulas, Y.; Huth, A.; Kraft, S.; Middleton, E.M.; Mohammed, G.; Nedbal, L.; et al. The FLuorescence EXplorer Mission Concept-ESA's Earth Explorer 8. *IEEE Trans. Geosci. Remote Sens.* **2017**, *55*, 1273–1284. [CrossRef]

93. Frankenberg, C.; Berry, J. Solar Induced Chlorophyll Fluorescence: Origins, Relation to Photosynthesis and Retrieval. In *Comprehensive Remote Sensing*; Liang, S., Ed.; Elsevier: Oxford, UK, 2018; pp. 143–162.
94. Rascher, U.; Alonso, L.; Burkart, A.; Cilia, C.; Cogliati, S.; Colombo, R.; Damm, A.; Drusch, M.; Guanter, L.; Hanus, J.; et al. Sun-induced fluorescence—A new probe of photosynthesis: First maps from the imaging spectrometer HyPlant. *Glob. Chang. Biol.* **2015**, *21*, 4673–4684. [CrossRef] [PubMed]
95. Porcar-Castell, A.; Tyystjärvi, E.; Atherton, J.; Van der Tol, C.; Flexas, J.; Pfündel, E.E.; Moreno, J.; Frankenberg, C.; Berry, J.A. Linking chlorophyll a fluorescence to photosynthesis for remote sensing applications: Mechanisms and challenges. *J. Exp. Bot.* **2014**, *65*, 4065–4095. [CrossRef] [PubMed]
96. Yang, P.; van der Tol, C.; Verhoef, W.; Alexander, D.; Anke, S.; Thorsten, K.; Onno, M.; Uwe, R. Using reflectance to explain vegetation biochemical and structural effects on sun-induced chlorophyll fluorescence. *Remote Sens. Environ.* **2019**, *231*, 110996. [CrossRef]
97. Gamon, J.A.; Penuelas, J.; Field, C.B. A narrow-waveband spectral index that tracks diurnal changes in photosynthetic efficiency. *Remote Sens. Environ.* **1992**, *41*, 35–44. [CrossRef]
98. Magney, T.S.; Vierling, L.A.; Eitel, J.U.H.; Huggins, D.R.; Garrity, S.R. Response of high frequency photochemical reflectance index (PRI) measurements to environmental conditions in wheat. *Remote Sens. Environ.* **2016**, *173*, 84–97. [CrossRef]
99. Zarco-Tejada, P.J.; González-Dugo, V.; Williams, L.E.; Suárez, L.; Berni, J.A.J.; Goldhamer, D.; Fereres, E. A PRI-based water stress index combining structural and chlorophyll effects: Assessment using diurnal narrow-band airborne imagery and the CWSI thermal index. *Remote Sens. Environ.* **2013**, *138*, 38–50. [CrossRef]
100. Ni, Z.; Liu, Z.; Huo, H.; Li, Z.L.; Nerry, F.; Wang, Q.; Li, X. Early water stress detection using leaf-level measurements of chlorophyll fluorescence and temperature data. *Remote Sens.* **2015**, *7*, 3232–3249. [CrossRef]
101. Yoshida, Y.; Joiner, J.; Tucker, C.; Berry, J.; Lee, J.-E.; Walker, G.; Reichle, R.; Koster, R.; Lyapustin, A.; Wang, Y. The 2010 Russian drought impact on satellite measurements of solar-induced chlorophyll fluorescence: Insights from modeling and comparisons with parameters derived from satellite reflectance. *Remote Sens. Environ.* **2015**, *166*, 163–177. [CrossRef]
102. Zarco-Tejada, P.J.; González-Dugo, V.; Berni, J.A.J. Fluorescence, temperature and narrow-band indices acquired from a UAV platform for water stress detection using a micro-hyperspectral imager and a thermal camera. *Remote Sens. Environ.* **2012**, *117*, 322–337. [CrossRef]
103. Zhao, W.; Liu, L.; Shen, Q.; Yang, J.; Han, X.; Tian, F.; Wu, J. Effects of Water Stress on Photosynthesis, Yield, and Water Use Efficiency in Winter Wheat. *Water* **2020**, *12*, 2127. [CrossRef]
104. Distelfeld, A.; Avni, R.; Fischer, A.M. Senescence, nutrient remobilization, and yield in wheat and barley. *J. Exp. Bot.* **2014**, *65*, 3783–3798. [CrossRef] [PubMed]
105. Montazeaud, G.; Karatoğma, H.; Özturk, I.; Roumet, P.; Ecarnot, M.; Crossa, J. Predicting wheat maturity and stay–green parameters by modeling spectral reflectance measurements and their contribution to grain yield under rainfed conditions. *Field Crop. Res.* **2016**, *196*, 191–198. [CrossRef]
106. Borrás, L.; Slafer, G.A.; Otegui, M.E. Seed dry weight response to source–sink manipulations in wheat, maize and soybean: A quantitative reappraisal. *Field Crop. Res.* **2004**, *86*, 131–146. [CrossRef]
107. Lim, P.O.; Kim, H.J.; Nam, H.G. Leaf senescence. *Annu. Rev. Plant Biol.* **2007**, *58*, 115–136. [CrossRef]
108. Crain, J.; Reynolds, M.; Poland, J. Utilizing high-throughput phenotypic data for improved phenotypic selection of stress-adaptive traits in wheat. *Crop Sci.* **2017**, *57*, 648. [CrossRef]
109. Lopes, M.S.; Reynolds, M.P. Stay-green in spring wheat can be determined by spectral reflectance measurements (normalized difference vegetation index) independently from phenology. *J. Exp. Bot.* **2012**, *63*, 3789–3798. [CrossRef]
110. Kipp, S.; Mistele, B.; Schmidhalter, U. Identification of stay-green and early senescence phenotypes in high-yielding winter wheat, and their relationship to grain yield and grain protein concentration using high-throughput phenotyping techniques. *Funct. Plant Biol.* **2014**, *41*, 227–235. [CrossRef]
111. Yang, J.; Zhang, J. Grain filling of cereals under soil drying. *New Phytol.* **2006**, *169*, 223–236. [CrossRef]
112. Gaju, O.; Allard, V.; Martre, P.; Le Gouis, J.; Moreau, D.; Bogard, M. Nitrogen partitioning and remobilization in relation to leaf senescence, grain yield and grain nitrogen concentration in wheat cultivars. *Field Crop. Res.* **2014**, *155*, 213–223. [CrossRef]
113. Cormier, F.; Foulkes, J.; Hirel, B.; Gouache, D.; Moënne-Loccoz, Y.; Le Gouis, J. Breeding for increased nitrogen-use efficiency: A review for wheat (*Triticum aestivum* L.). *Plant Breed.* **2016**, *135*, 255–278. [CrossRef]
114. Blatt, M.R. Ca^{2+} signalling and control of guard-cell volume in stomatal movements. Blatt MR. *Curr. Opin. Plant Biol.* **2000**, *3*, 196–204. [CrossRef]
115. Grill, E.; Himmelbach, A. ABA signal transduction. *Curr. Opin. Plant Biol.* **1998**, *1*, 412–418. [CrossRef]
116. Vadivambal, R.; Jayas, D.S. Applications of Thermal Imaging in Agriculture and Food Industry—A Review. *Food Bioprocess Technol.* **2010**, *4*, 186–199. [CrossRef]
117. Palazzi, V.; Bonafoni, S.; Alimenti, F.; Mezzanotte, P.; Roselli, L. Feeding the World with Microwaves: How Remote and Wireless Sensing Can Help Precision Agriculture. *IEEE Microw. Mag.* **2019**, *20*, 72–86. [CrossRef]
118. Gonzalez-Dugo, V.; Zarco-Tejada, P.; Nicolás, E.; Nortes, P.A.; Alarcón, J.J.; Intrigliolo, D.S.; Fereres, E. Using high resolution UAV thermal imagery to assess the variability in the water status of five fruit tree species within a commercial orchard. *Precis. Agric.* **2013**, *14*, 660–678. [CrossRef]

119. Osroosh, Y.; Troy Peters, R.; Campbell, C.S.; Zhang, Q. Automatic irrigation scheduling of apple trees using theoretical crop water stress index with an innovative dynamic threshold. *Comput. Electron. Agric.* **2015**, *118*, 193–203. [CrossRef]
120. Ribeiro-Gomes, K.; Hernández-López, D.; Ortega, J.; Ballesteros, R.; Poblete, T.; Moreno, M. Uncooled Thermal Camera Calibration and Optimization of the Photogrammetry Process for UAV Applications in Agriculture. *Sensors* **2017**, *17*, 2173. [CrossRef]
121. Idso, S.B.; Reginato, R.J.; Hatfield, J.L.; Walker, G.K.; Jackson, R.D.; Pinter, P.J. A generalization of the stress-degree-day concept of yield prediction to accommodate a diversity of crops. *Agric. Meteorol.* **1980**, *21*, 205–211. [CrossRef]
122. Ghazouani, H.; Capodici, F.; Ciraolo, G.; Maltese, A.; Rallo, G.; Provenzano, G. Potential of thermal images and simulation models to assess water and salt stress: Application to potato crop in central Tunisia. *Chem. Eng. Trans.* **2017**, *58*, 709–714. [CrossRef]
123. Cohen, Y.; Alchanatis, V.; Meron, M.; Saranga, S.; Tsipris, J. Estimation of leaf water potential by thermal imagery and spatial analysis. *J. Exp. Bot.* **2005**, *56*, 1843–1852. [CrossRef] [PubMed]
124. Fuchs, M. Infrared measurement of canopy temperature and detection of plant water stress. *Theor. Appl. Climatol.* **1990**, *42*, 253–261. [CrossRef]
125. Jones, H.G.; Stoll, M.; Santos, T.; de Sousa, C.; Chaves, M.M.; Grant, O.M. Use of infrared thermometry for monitoring stomatal closure in the field: Application to grapevine. *J. Exp. Bot.* **2002**, *53*, 2240–2260. [CrossRef]
126. Moran, M.S.; Clarke, T.R.; Inoue, Y.; Vidal, A. Estimating crop water deficit using the relation between surface-air temperature and spectral vegetation index. *Remote Sens. Environ.* **1994**, *49*, 246–263. [CrossRef]
127. Inoue, Y.; Sakuratani, T.; Shibayama, M.; Morinaga, S. Remote and real-time sensing of canopy transpiration and conductance: Comparison of remote and stem flow gauge methods in soybean canopies as affected by soil water status. *Jpn. J. Crop Sci.* **1994**, *63*, 664–670. [CrossRef]
128. Labbé, S.; Lebourgeois, V.; Jolivot, A.; Marti, R. Thermal infra-red remote sensing for water stress estimation in agriculture. In *The use of Remote Sensing and Geographic Information Systems for Irrigation Management in Southwest Europe. Zaragoza: CIHEAM/IMIDA/SUDOE Interreg IVB (EU-ERDF)*; Erena, M., López-Francos, A., Montesinos, S., Berthoumieu, J.-P., Eds.; (Options Méditerranéennes: Série B. Etudes et Recherches; n. 67); CIHEAM/IMIDA/SUDOE Interreg IVB (EU-ERDF): Zaragoza, Spain, 2012; pp. 175–184. Available online: https://om.ciheam.org/om/pdf/b67/00006607.pdf (accessed on 16 July 2021).
129. Lebourgeois, V.; Labbé, S.; Bégué, A.; Jacob, F. Atmospheric corrections of low altitude thermal airborne images acquired over a tropical cropped area. In Proceedings of the IEEE International Geoscience and Remote Sensing Symposium, Boston, MA, USA, 6–11 July 2008.
130. Sobrino, J.A.; Del Frate, F.; Drusch, M.; Jimenez-Munoz, J.C.; Manunta, P.; Regan, A. Review of Thermal Infrared Applications and Requirements for Future High-Resolution Sensors. *IEEE Trans. Geosci. Remote Sens.* **2016**, *54*, 2963–2972. [CrossRef]
131. Berni, J.; Zarco-Tejada, P.J.; Suarez, L.; Fereres, E. Thermal and Narrowband Multispectral Remote Sensing for Vegetation Monitoring from an Unmanned Aerial Vehicle. *IEEE Trans. Geosci. Remote Sens.* **2009**, *47*, 722–738. [CrossRef]
132. Raoufi, R.; Beighley, E. Estimating Daily Global Evapotranspiration Using Penman–Monteith Equation and Remotely Sensed Land Surface Temperature. *Remote Sens.* **2017**, *9*, 1138. [CrossRef]
133. Khanal, S.; Fulton, J.; Shearer, S. An overview of current and potential applications of thermal remote sensing in precision agriculture. *Comput. Electron. Agric.* **2017**, *139*, 22–32. [CrossRef]
134. Nugraha, A.S.A.; Gunawan, T.; Kamal, M. Downscaling land surface temperature on multi-scale image for drought monitoring. In Proceedings of the Sixth Geoinformation Science Symposium, Yogyakarta, Indonesia, 21 November 2019. [CrossRef]
135. Hoffmann, H.; Jensen, R.; Thomsen, A.; Nieto, H.; Rasmussen, J.; Friborg, T. Crop water stress maps for an entire growing season from visible and thermal UAV imagery. *Biogeosciences* **2016**, *13*, 6545–6563. [CrossRef]
136. Zha, Q.; Xi, X.; He, Y.; Jiang, A. Transcriptomic analysis of the leaves of two grapevine cultivars under high-temperature stress. *Sci. Hortic.* **2020**, *265*, 109265. [CrossRef]
137. Sandholt, I.; Rasmussen, K.; Andersen, J. A simple interpretation of the surface temperature/vegetation index space for assessment of surface moisture status. *Remote Sens. Environ.* **2002**, *79*, 213–224. [CrossRef]
138. Dhungel, R.; Aiken, R.; Colaizzi, P.D.; Lin, X.; Baumhardt, R.L.; Evett, S.R.; Brauer, D.K.; Marek, G.W.; O'Brien, D. Increased Bias in Evapotranspiration Modeling Due to Weather and Vegetation Indices Data Sources. *Agron. J.* **2019**, *111*, 1407–1424. [CrossRef]
139. Heinemann, S.; Siegmann, B.; Thonfeld, F.; Muro, J.; Jedmowski, C.; Kemna, A.; Kraska, T.; Muller, O.; Schultz, J.; Udelhoven, T.; et al. Land Surface Temperature Retrieval for Agricultural Areas Using a Novel UAV Platform Equipped with a Thermal Infrared and Multispectral Sensor. *Remote Sens.* **2020**, *12*, 1075. [CrossRef]
140. Ciężkowski, W.; Szporak-Wasilewska, S.; Kleniewska, M.; Jóźwiak, J.; Gnatowski, T.; Dąbrowski, P.; Góraj, M.; Szatyłowicz, J.; Ignar, S.; Chormański, J. Remotely Sensed Land Surface Temperature-Based Water Stress Index for Wetland Habitats. *Remote Sens.* **2020**, *12*, 631. [CrossRef]
141. Malbéteau, Y.; Parkes, S.; Aragon, B.; Rosas, J.; McCabe, M. Capturing the Diurnal Cycle of Land Surface Temperature Using an Unmanned Aerial Vehicle. *Remote Sens.* **2018**, *10*, 1407. [CrossRef]
142. Torres-Rua, A.F.; Aboutalebi, M.; Wright, T.; Nassar, A.; Guillevic, P.; Hipps, L.; Gao, F.; Jim, K.; Alsina, M.M.; Coopmans, C.; et al. Estimation of surface thermal emissivity in a vineyard for UAV microbolometer thermal cameras using NASA HyTES hyperspectral thermal, and landsat and AggieAir optical data. In *Autonomous Air and Ground Sensing Systems for Agricultural Optimization and Phenotyping IV*; Proceedings Volume 11008, SPIE Defense + Commercial Sensing; International Society for Optics and Photonics: Baltimore, MD, USA, 2019. [CrossRef]

143. Jay, S.; Comar, A.; Benicio, R.; Beauvois, J.; Dutartre, D.; Daubige, G.; Li, W.; Labrosse, J.; Thomas, S.; Henry, N.; et al. Scoring Cercospora Leaf Spot on Sugar Beet: Comparison of UGV and UAV Phenotyping Systems. *Plant Phenomics* **2020**, *2020*, 9452123. [CrossRef]
144. El-Shirbeny, M.A.; Saleh, S.M. Actual evapotranspiration evaluation based on multi-sensed data. *J. Arid. Agric.* **2021**, 95–102. [CrossRef]
145. Jones, H.G.; Schofield, P. Thermal and other remote sensing of plant stress. *Gen. Appl. Plant Physiol.* **2008**, *34*, 19–32. Available online: https://citeseerx.ist.psu.edu/viewdoc/download?doi=10.1.1.399.2918&rep=rep1&type=pdf (accessed on 16 July 2021).
146. Meron, M.; Tsipris, J.; Orlov, V.; Alchanatis, V.; Cohen, Y. Crop water stress mapping for site-specific irrigation by thermal imagery and artificial reference surfaces. *Precis. Agric.* **2010**, *11*, 148–162. [CrossRef]
147. Campbell, B.A. *Radar Remote Sensing of Planetary Surfaces*; Cambridge University Press: Cambridge, UK, 2002.
148. Okujeni, A.; Jänicke, C.; Cooper, S.; Frantz, D.; Hostert, P.; Clark, M.; Segl, K.; van der Linden, S. Multi-season unmixing of vegetation class fractions across diverse Californian ecoregions using simulated spaceborne imaging spectroscopy data. *Remote Sens. Environ.* **2021**, *2021*, 112558. [CrossRef]
149. Yu, X.; Hyyppä, J.; Litkey, P.; Kaartinen, H.; Vastaranta, M.; Holopainen, M. Single-Sensor Solution to Tree Species Classification Using Multispectral Airborne Laser Scanning. *Remote Sens.* **2017**, *9*, 108. [CrossRef]
150. Ibrahim, E.; Monbaliu, J. Suitability of spaceborne multispectral data for inter-tidal sediment characterization: A case study. Estuarine. *Coast. Shelf Sci.* **2011**, 92437–92445. [CrossRef]
151. Navarro, A.; Rolim, J.; Miguel, I.; Catalão, J.; Silva, J.; Painho, M.; Vekerdy, Z. Crop Monitoring Based on SPOT-5 Take-5 and Sentinel-1A Data for the Estimation of Crop Water Requirements. *Remote Sens.* **2016**, *8*, 525. [CrossRef]
152. Kukkonen, M.; Maltamo, M.; Korhonen, L.; Packalen, P. Multispectral Airborne LiDAR Data in the Prediction of Boreal Tree Species Composition. *IEEE Trans. Geosci. Remote Sens.* **2019**, *57*, 3462–3471. [CrossRef]
153. Hopkinson, C.; Chasmer, L.; Gynan, C.; Mahoney, C.; Sitar, M. Multisensor and Multispectral LiDAR Characterization and Classification of a Forest Environment. *Can. J. Remote Sens.* **2016**, 42501–42520. [CrossRef]
154. Teo, T.A.; Wu, H.M. Analysis of Land Cover Classification Using Multi-Wavelength LiDAR System. *Appl. Sci.* **2017**, *7*, 663. [CrossRef]
155. Bakuła, K.; Kupidura, P.; Jełowicki, L. Testing of Land Cover Classifacation from Multispectral Airborne Laser Scanning Data. Remote Sensing and Spatial Information Sciences, Prague, Czech Republic. *Int. Arch. Photogramm.* **2016**, *41*, 161–169.
156. Matikainen, L.; Karila, K.; Hyyppä, J.; Litkey, P.; Puttonen, E.; Ahokas, E. Object-based analysis of multispectral airborne laser scanner data for land cover classification and map updating. *ISPRS J. Photogramm. Remote Sens.* **2017**, *128*, 298–313. [CrossRef]
157. Ahokas, E.; Hyyppä, J.; Yu, X.; Liang, X.; Matikainen, L.; Karila, K.; Litkey, P.; Kukko, A.; Jaakkola, A.; Kaartinen, H.; et al. Towards Automatic Single-Sensor Mapping by Multispectral Airborne Laser Scanning. Remote Sensing and Spatial Information Sciences, Prague. *Czech Repub. Int. Arch. Photogramm.* **2016**, *41*, 155–162.
158. Pinter, P.J., Jr.; Hatfield, J.L.; Schepers, J.S.; Barnes, E.M.; Moran, M.S.; Daughtry, C.S.; Upchurch, D.R. Remote Sensing for Crop Management. *Photogramm. Eng. Remote Sens.* **2003**, *69*, 647–664. [CrossRef]
159. Timmermans, J.; Buitrago-Acevedo, M.; Corbin, A.; Verhoef, W. Auto-correcting for atmospheric effects in thermal hyperspectral measurements. *Int. J. Appl. Earth Obs. Geoinf.* **2018**, *71*, 20–28. [CrossRef]
160. Kealy, P.S.; Hook, S.J. Separating temperature and emissivity in thermal infrared multispectral scanner data: Implications for recovering land surface temperatures. *IEEE Trans. Geosci. Remote Sens.* **1993**, *31*, 1155–1164. [CrossRef]
161. Schmugge, T.; French, A.; Ritchie, J.C.; Rango, A.; Pelgrum, H. Temperature and emissivity separation from multispectral thermal infrared observations. *Remote Sens. Environ.* **2002**, *79*, 189–198. [CrossRef]
162. Fu, Y.; Yang, G.; Pu, R.; Li, Z.; Li, H.; Xu, X.; Song, X.; Yang, X.; Zhao, C. An overview of crop nitrogen status assessment using hyperspectral remote sensing: Current status and perspectives. *Eur. J. Agron.* **2021**, *124*, 126241. [CrossRef]
163. Alordzinu, K.E.; Li, J.; Lan, Y.; Appiah, S.A.; AL Aasmi, A.; Wang, H.; Liao, J.; Sam-Amoah, L.K.; Qiao, S. Ground-Based Hyperspectral Remote Sensing for Estimating Water Stress in Tomato Growth in Sandy Loam and Silty Loam Soils. *Sensors* **2021**, *21*, 5705. [CrossRef] [PubMed]
164. Ribeiro da Luz, B.; Crowley, J.K. Spectral reflectance and emissivity features of broad leaf plants: Prospects for remote sensing in the thermal infrared (8.0–14.0 µm). *Remote Sens. Environ.* **2007**, *109*, 393–405. [CrossRef]
165. Galvao, L.S.; Epiphanio, J.C.N.; Breuning, F.M.; Formaggio, A.R. Crop type discrimination using hyperspectral data. In *Hyperspectral Remote Sensing of Vegetation*; Thenkabail, P.S., Lyon, J.G., Huete, A., Eds.; CRC Press: Boca Raton, FL, USA, 2012; pp. 397–422.
166. Rock, G.; Gerhards, M.; Schlerf, M.; Hecker, C.; Udelhoven, T. Plant species discrimination using emissive thermal infrared imaging spectroscopy. *Int. J. Appl. Earth Obs. Geoinf.* **2016**, *53*, 16–26. [CrossRef]
167. Gerhards, M.; Rock, G.; Schlerf, M.; Udelhoven, T. Water stress detection in potato plants using leaf temperature, emissivity, and reflectance. *Int. J. Appl. Earth Obs. Geoinf.* **2016**, *53*, 27–39. [CrossRef]
168. Buitrago, M.F.; Groen, T.A.; Hecker, C.A.; Skidmore, A.K. Changes in thermal infrared spectra of plants caused by temperature and water stress. *ISPRS J. Photogramm. Remote Sens.* **2016**, *111*, 22–31. [CrossRef]
169. Buitrago Acevedo, M.F.; Groen, T.A.; Hecker, C.A.; Skidmore, A.K. Identifying leaf traits that signal stress in TIR spectra. *ISPRS J. Photogramm. Remote Sens.* **2017**, *125*, 132–145. [CrossRef]

170. Koetz, B.; Berger, M.; Blommaert, J.; Del Bello, U.; Drusch, M.; Duca, R.; Gascon, F.; Ghent, D.; Hoogeveen, J.; Hook, S.; et al. Copernicus High Spatio-Temporal Resolution Land Surface Temperature Mission: Mission Requirements Document. Published in 2019. Available online: http://esamultimedia.esa.int/docs/EarthObservation/Copernicus_LSTM_MRD_v2.0_Issued20190308.pdf (accessed on 16 July 2021).
171. Abrams, M.J.; Hook, S.J. NASA's Hyperspectral Infrared Imager (HyspIRI). In *Thermal Infrared Remote Sensing*; Kuenzer, C., Dech, S., Eds.; Remote Sensing and Digital Image Processing; Springer: Dordrecht, The Netherlands, 2013; Volume 17, pp. 117–130.
172. Udelhoven, T.; Schlerf, M.; Segl, K.; Mallick, K.; Bossung, C.; Retzlaff, R.; Rock, G.; Fischer, P.; Müller, A.; Storch, T.; et al. A Satellite-Based Imaging Instrumentation Concept for Hyperspectral Thermal Remote Sensing. *Sensors* **2017**, *17*, 1542. [CrossRef]
173. Grant, O.M.; Davies, M.J.; James, C.M.; Johnson, A.W.; Leinonen, I.; Simpson, D.W. Thermal imaging and carbon isotope composition indicate variation amongst strawberry (Fragaria×ananassa) cultivars in stomatal conductance and water use efficiency. *Environ. Exp. Bot.* **2012**, *76*, 7–15. [CrossRef]
174. Kim, Y.; Evans, R.G.; Iversen, W.M. Remote sensing and control of an irrigation system using a distributed wireless sensor network. *IEEE Trans. Instrum. Meas.* **2008**, *57*, 1379–1387.
175. Gutiérrez, J.; Villa-Medina, J.F.; Nieto-Garibay, A.; Porta-Gándara, M.Á. Automated irrigation system using a wireless sensor network and gprs module. *IEEE Trans. Instrum. Meas.* **2013**, *63*, 166–176. [CrossRef]
176. Evett, S.; O'Shaughnessy, S.A.; Andrade, M.A.; Colaizzi, P.; Schwartz, R.C.; Schomberg, H.S.; Stone, K.C.; Vories, E.D.; Sui, R. Theory and Development of a VRI Decision Support System: The USDA-ARS ISSCADA Approach. *Trans. ASABE* **2020**, *63*, 1507–1519. [CrossRef]
177. O'Shaughnessy, S.A.; Evett, S.R.; Colaizzi, P.D.; Howell, T.A. Wireless Sensor Network Effectively Controls Center Pivot Irrigation of Sorghum. *Appl. Eng. Agric.* **2013**, 29853–29864. [CrossRef]
178. Andrade, M.A.; Shaughnessy, S.A.O.; Evett, S.R. ARSmartPivot v-1—Sensor based management software for center pivot irrigation systems. In Proceedings of the ASABE Annual International Meeting, New Orleans, Louisiana, 26–29 July 2015. [CrossRef]
179. Andrade, M.A.; Shaughnessy, S.A.O.; Evett, S.R. ARSPIVOT, A sensor-based Decision Support Tool for the Integrated irrigation Management of VRI Center Pivot Systems, Oak Ridge Institute for Science and Education Sponsored by USDA-ARS. In USDA-ARS USDA-ARS. In Proceedings of the 28th Annual Central Plains Irrigation Conference, Burlington, CO, USA, 21–22 February 2017.
180. O'Shaughnessy, S.A.; Andrade, M.A.; Evett, S.R. Using an integrated crop water stress index for irrigation scheduling of two corn hybrids in a semi-arid region. *Irrig. Sci.* **2017**, *35*, 31451–31467. [CrossRef]
181. Lee, W.; Alchanatis, V.; Yang, C.; Hirafuji, M.; Moshou, D.; Li, C. Sensing technologies for precision specialty crop production. *Comput. Electron. Agric.* **2010**, *74*, 2–33. [CrossRef]
182. Ramos-Giraldo, P.; Reberg-Horton, C.; Locke, A.M.; Mirsky, S.; Lobaton, E. Drought Stress Detection Using Low-Cost Computer Vision Systems and Machine Learning Techniques. *IT Prof.* **2020**, *22*, 27–29. [CrossRef]
183. Singh, A.K.; Ganapathysubramanian, B.; Sarkar, S.; Singh, A. Deep learning for plant stress phenotyping: Trends and future perspectives. *Trends Plant Sci.* **2018**, *23*, 10–883. [CrossRef]
184. Shakoor, N.; Lee, S.; Mockler, T.C. High throughput phenotyping to accelerate crop breeding and monitoring of diseases in the field. *Curr. Opin. Plant Biol.* **2017**, *38*, 184–192. [CrossRef]
185. Chandel, N.S.; Chakraborty, S.K.; Rajwade, Y.A.; Dubey, K.; Tiwari, M.K.; Jat, D. Identifying crop water stress using deep learning models. *Neural Comput. Appl.* **2021**, *33*, 5353–5367. [CrossRef]
186. Carter, G.A. Primary and secondary effects of water content on the spectral reflectance of leaves. *Am. J. Bot.* **1991**, *78*, 916–924. [CrossRef]
187. Oumar, Z.; Mutanga, O. Predicting water stress induced by Thaumastocoris peregrinus infestations in plantation forests using field spectroscopy and neural networks. *J. Spat. Sci.* **2014**, *59*, 79–90. [CrossRef]
188. Zeyliger, A.M.; Ermolaeva, O.S. Water Stress Regime of Irrigated Crops Based on Remote Sensing and Ground-Based Data. *Agronomy* **2021**, *11*, 1117. [CrossRef]
189. Elsayed, S.; Darwish, W. Hyperspectral remote sensing to assess the water status, biomass, and yield of maize cultivars under salinity and water stress. *Bragantia Scielo Br.* **2017**, *76*, 62–72. [CrossRef]
190. Li, H.; Yang, W.; Lei, J.; She, J.; Zhou, X. Estimation of leaf water content from hyperspectral data of different plant species by using three new spectral absorption indices. *PLoS ONE* **2021**, *16*, e0249351. [CrossRef]
191. Eitel, J.U.; Magney, T.S.; Vierling, L.A.; Brown, T.T.; Huggins, D.R. LiDAR based biomass and crop nitrogen estimates for rapid, non-destructive assessment of wheat nitrogen status. *Field Crops Res.* **2014**, *159*, 21–32. [CrossRef]
192. Guo, Q.; Wu, F.; Pang, S.; Zhao, X.; Chen, L.; Liu, J.; Xue, B.; Xu, G.; Li, L.; Jing, H. Crop 3D—a LiDAR based platform for 3D high-throughput crop phenotyping. *Sci. China Life Sci.* **2018**, *61*, 328–339. [CrossRef]
193. Jin, S.; Su, Y.; Wu, F.; Pang, S.; Gao, S.; Hu, T.; Liu, J.; Guo, Q. Stem-leaf segmentation and phenotypic trait extraction of individual maize using terrestrial LiDAR data. *IEEE Trans Geosci. Remote Sens.* **2018**, *2*, 1. [CrossRef]
194. Sanz, R.; Rosell, J.R.; Llorens, J.; Gil, E.; Planas, S. Relationship between tree row LIDAR-volume and leaf area density for fruit orchards and vineyards obtained with a LIDAR 3D Dynamic Measurement System. *Agric. For. Meteorol.* **2013**, *171*, 153–162. [CrossRef]
195. Walter, J.D.C.; Edwards, J.; McDonald, G.; Kuchel, H. Estimating Biomass and Canopy Height with LiDAR for Field Crop Breeding. *Front. Plant Sci.* **2019**, *10*, 1145. [CrossRef] [PubMed]

196. Lin, Y. LiDAR: An important tool for next-generation phenotyping technology of high potential for plant phenomics? *Comput. Electron. Agric.* **2015**, *119*, 61–73. [CrossRef]
197. Roth, B.D.; Goodenough, A.A.; Brown, S.D.; van Aardt, J.A.; Saunders, M.G.; Krause, K. Simulations of Leaf BSDF Effects on Lidar Waveforms. *Remote Sens.* **2020**, *12*, 2909. [CrossRef]
198. Shen, X.; Cao, L.; Coops, N.C.; Fan, H.; Wu, X.; Liu, H.; Wang, G.; Cao, F. Quantifying vertical profiles of biochemical traits for forest plantation species using advanced remote sensing approaches. *Remote Sens. Environ.* **2020**, *250*, 112041. [CrossRef]
199. An, J.; Li, W.; Li, M.; Cui, S.; Yue, H. Identification and classification of maize drought stress using deep convolutional neural network. *Symmetry* **2019**, *11*, 256. [CrossRef]
200. Giménez-Gallego, J.; González-Teruel, J.D.; Jiménez-Buendía, M.; Toledo-Moreo, A.B.; Soto-Valles, F.; Torres-Sánchez, R. Segmentation of multiple tree leaves pictures with natural backgrounds using deep learning for image-based agriculture applications. *Appl. Sci.* **2020**, *10*, 202. [CrossRef]
201. Zhuang, S.; Wang, P.; Jiang, B.; Li, M. Learned features of leaf phenotype to monitor maize water status in the fields. *Comput. Electron. Agric.* **2020**, *172*, 10–1016. [CrossRef]
202. El-Shirbeny, M.A.; Ali, A.M.; Savin, I.; Poddubskiy, A.; Dokukin, P. Agricultural Water Monitoring for Water Management Under Pivot Irrigation System Using Spatial Techniques. *Earth Syst. Environ.* **2021**, *5*, 341–351. [CrossRef]
203. Herrero-Huerta, M.; Lagüela, S.; Alfieri, S.M.; Menenti, M. Generating high-temporal and spatial resolution TIR image data. International. *J. Appl. Earth Obs. Geoinf.* **2019**, *78*, 149–162. [CrossRef]
204. Inglada, J.; Vincent, A.; Arias, M.; Marais-Sicre, C. Improved Early Crop Type Identification by Joint Use of High Temporal Resolution SAR and Optical Image Time Series. *Remote Sens.* **2016**, *8*, 362. [CrossRef]
205. Cui, Y.; Chen, X.; Xiong, W.; He, L.; Lv, F.; Fan, W.; Luo, Z.; Hong, Y. A Soil Moisture Spatial and Temporal Resolution Im-proving Algorithm Based on Multi-Source Remote Sensing Data and GRNN Model. *Remote Sens.* **2020**, *12*, 455. [CrossRef]